

---

# Learning Dynamic Knowledge Graphs to Generalize on Text-Based Games

---

Ashutosh Adhikari<sup>\*1</sup> Xingdi Yuan<sup>\*2</sup> Marc-Alexandre Côté<sup>\*2</sup> Mikuláš Zelinka<sup>3</sup> Marc-Antoine Rondeau<sup>2</sup>  
 Romain Laroche<sup>2</sup> Pascal Poupart<sup>14</sup> Jian Tang<sup>56</sup> Adam Trischler<sup>2</sup> William L. Hamilton<sup>57</sup>

## Abstract

Playing text-based games requires skill in processing natural language and in planning. Although a key goal for agents solving this task is to generalize across multiple games, most previous work has either focused on solving a single game or has tackled generalization with rule-based heuristics. In this work, we investigate how structured information in the form of a knowledge graph (KG) can facilitate effective planning and generalization. We introduce a novel transformer-based sequence-to-sequence model that constructs a “belief” KG from raw text observations of the environment, dynamically updating this belief graph at every game step as it receives new observations. To train this model to build useful graph representations, we introduce and analyze a set of graph-related pre-training tasks. We demonstrate empirically that KG-based representations from our model help agents to converge faster to better policies for multiple text-based games, and further, enable stronger zero-shot performance on unseen games. Experiments on unseen games show that our best agent outperforms text-based baselines by 21.6%.

## 1. Introduction

Language is at the core of many human interactions, especially when interactions involve the transfer of knowledge. Consider recording information in written text, extracting information from text by reading, communicating with other humans, and so on. We expect intelligent agents to have the ability to interact with the human world either in reality (e.g., customer service systems) or in simulated environments (e.g., video games). Therefore, it makes sense to teach agents to interact through language.

<sup>\*</sup>Equal contribution. <sup>1</sup>University of Waterloo <sup>2</sup>Microsoft Research, Montréal <sup>3</sup>Charles University <sup>4</sup>Vector Institute <sup>5</sup>Mila <sup>6</sup>HEC Montréal <sup>7</sup>McGill University. Correspondence to: Xingdi Yuan <eric.yuan@microsoft.com>.

Text-based games are complex interactive simulations in which the game state is described with text and players interact using simple text commands (e.g., **light torch with match**). These games are a great proxy for studying how agents can exploit language to interact with the environment. Solving them requires a combination of reinforcement learning (RL) and natural language processing (NLP) techniques. However, due to inherent challenges like partial observability, long-term dependencies, reward sparsity, and combinatorial action spaces, these games are extremely difficult to solve.<sup>1</sup> As a testament to this challenge, Hausknecht et al. (2019b) show that a state-of-the-art model achieves a mere 2.56% of the total possible score on a curated set of text-based games (Atkinson et al., 2018).

Most previous work has approached text-based games by developing learning agents that solve a single game, without testing for generalization (Narasimhan et al., 2015; He et al., 2015; Fulda et al., 2017; Zahavy et al., 2018). Others have designed rule-based components that prune the action space or shape the rewards in ways that rely on *a priori* knowledge of the game dynamics (Yuan et al., 2018; Lima, 2019; Adolphs & Hofmann, 2019; Yin & May, 2019b). A more recent line of work (Ammanabrolu & Riedl, 2018; Ammanabrolu & Hausknecht, 2020) takes advantage of the structured nature of text-based games by building knowledge graph (KG) representations of the game state. Those methods use heuristics to populate a KG that feeds into a deep network. However, to learn general representations and policies for playing games, we expect it is necessary to build agents that learn and scale more automatically, replacing heuristics with learning (Sutton, 2019).

This work investigates methods for learning general policies for text-based games focusing on graph-structured state representations. We hypothesize that encoding text-based state descriptions as KGs will foster better training convergence and test performance across *multiple games*. To test this hypothesis, we propose the Graph Aided Transformer Agent (GATA)<sup>2</sup>. GATA is a deep neural model that, in lieu

<sup>1</sup>We challenge readers to solve this representative game: <https://aka.ms/textworld-tryit>.

<sup>2</sup>Code: <https://github.com/xingdi-eric-yuan/GATA-public>

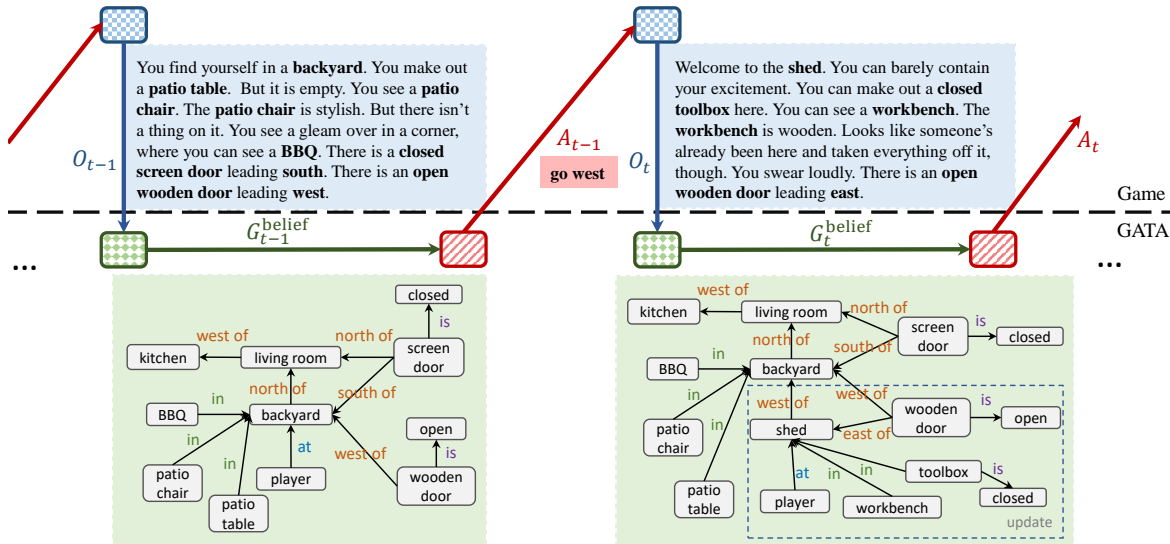


Figure 1. GATA playing a text-based game by updating its belief graph. In response to action  $A_{t-1}$ , the environment returns text observation  $O_t$ . Based on  $O_t$  and  $G_{t-1}^{\text{belief}}$ , the agent updates  $G_t^{\text{belief}}$  and selects a new action  $A_t$ . In the figure, blue box with squares is the game engine, green box with diamonds is the graph updater, red box with slashes is the action selector.

of hand-crafted heuristics, *learns* to construct and update its belief state<sup>3</sup> in the form of a dynamic knowledge graph.

We benchmark the agents studied in this work on 500+ unique games generated by TextWorld (Côté et al., 2018), distributed across four difficulty levels. To glean concrete insights on the effects of graph-structured representations on performance and generalization, we conduct incremental experiments. First, we relax the challenge of partial observability by providing to GATA the full ground-truth KG that describes the current game state. Next, we provide a partial view of the full KG that contains only the ground-truth information encountered by the agent up to its current time step. Finally, and most interestingly, we ask our agent to construct and update its own KG entirely from raw text observations. Experimental results show that GATA leverages KGs to learn more effectively on multiple games and to generalize better to unseen games, supporting our hypothesis.

The main contributions of this work are as follows:

1. We conduct thorough experimental analyses showing structured knowledge representations (KGs) to yield better training performance and **zero-shot generalization** in text-based games.
2. We propose a novel agent, GATA, that constructs and updates an internal **graph-structured belief** of the world from text observations and uses this to play text-based games.
3. We show that **self-supervised graph representation**

<sup>3</sup>Text-based games are partially observable environments.

**learning** can boost performance when used to pre-train GATA’s graph encoder.

## 2. Background

### 2.1. Text-based Games and KGs

Text-based games can be formally described as partially observable Markov decision processes (POMDP) (Côté et al., 2018). They are environments in which the player receives text-only observations describing the current observable state and interacts by issuing short phrases as actions (e.g., in Figure 1, *go west* moves the player to a new location). Usually, the end goal is not clear from the start. To figure it out, the player gets sparse reward for completing subgoals.

Text-based games broadly have two different settings: *parser-based*, where the player must generate text actions word by word, and *choice-based*, where the player chooses action  $A_t$  from a list of action candidates  $C_t$  at every game step  $t$ . Further, they have a variety of difficulty levels, which are determined mainly by the environment’s complexity (i.e., how many locations in the game, and how many objects are interactable), the game length (i.e., optimally, how many actions are required to win), and the verbosity (i.e., how much text information is irrelevant to solving the game).

In a text-based game, at any time step  $t$ , the game state  $S_t$  can be represented as a graph  $G_t^{\text{full}} = (\mathcal{V}_t, \mathcal{E}_t)$ . The vertices  $\mathcal{V}_t$  represent entities (including the player, objects, and locations) and their current conditions (e.g., closed, fried, sliced), while the edges  $\mathcal{E}_t$  represent relations between the entities (e.g., *north.of*, *in*, *is*). Given the partially

observable nature of the environment, we define  $\mathcal{G}_t^{\text{seen}}$  (a subgraph of  $\mathcal{G}_t^{\text{full}}$ ) that contains only the vertices and edges observable to the agent along its trajectory up to time  $t$ . The framework we use in this work, TextWorld, makes ground-truth graphs  $\mathcal{G}_t^{\text{full}}$  and  $\mathcal{G}_t^{\text{seen}}$  available (see Appendix E).

At every step  $t$ , a text-based game provides a text observation  $O_t$  that describes the information observable to an agent. We denote by  $\mathcal{G}_t^{\text{belief}}$  a belief graph, which represents the agent’s “belief” about the true game state according to what it has observed so far. At time step  $t$ , the agent updates the belief from  $\mathcal{G}_{t-1}^{\text{belief}}$  using  $O_t$ . Training our agent to construct and update  $\mathcal{G}_t^{\text{belief}}$  accurately is one of our ultimate goals. In the case where the agent’s language understanding and belief update procedure are flawless, we expect  $\mathcal{G}_t^{\text{belief}} = \mathcal{G}_t^{\text{seen}}$ . Figure 1 illustrates an agent in a text-based game updating  $\mathcal{G}_t^{\text{belief}}$  from  $O_t$  and then issuing an action  $\mathcal{A}_t$ .

In this work, we define a transition as a 7-tuple  $(\mathcal{G}_{t-1}, O_{t-1}, C_{t-1}, \mathcal{A}_{t-1}, \mathcal{G}_t, O_t, r_{t-1})$ . Specifically, given  $\mathcal{G}_{t-1}$  and  $O_{t-1}$ , an action  $\mathcal{A}_{t-1}$  is selected from the candidate list  $C_{t-1}$ ; this leads to a new game state  $\mathcal{S}_t$ , thus  $\mathcal{G}_t$  and  $O_t$  are returned with a reward  $r_{t-1} = R(\mathcal{S}_{t-1}, \mathcal{A}_{t-1})$ .  $R$  is a reward function. Note that  $\mathcal{G}_t$  in transitions can either be  $\mathcal{G}_t^{\text{full}}$  or  $\mathcal{G}_t^{\text{seen}}$ .

## 2.2. Problem Setting

In this work, we use TextWorld (Côté et al., 2018) to generate unique *choice-based* games of different difficulty levels that share the same overarching theme. An agent must gather and process ingredients, placed randomly across multiple locations, according to some recipe it discovers during the game. The agent earns a point for collecting each ingredient and for cutting and/or cooking it correctly. Upon completing the recipe, the game is won. However, wrongly processing any ingredient leads to game termination (e.g., **slice carrot** instead of **dice carrot**). To process ingredients, an agent also needs to access and utilize appropriate tools (e.g., a knife is required to **slice**, **dice**, or **chop**; a stove is used for frying, an oven for roasting). We generate training, validation, and test game sets, all of which have unique recipes and different map configurations. Adopting the standard supervised learning paradigm for evaluating generalization, we use the validation set for hyperparameter tuning and report performance on the test set.

Previously, Trischler et al. (2019) presented the *First TextWorld Problems (FTWP)* dataset, which consists of games that follow a cooking theme and with a wider range of difficulty levels. However, that dataset provides 10 games per difficulty level, which is insufficient for experiments centered on generalization.

Therefore, we generated a new set of games for this work. We use the *FTWP* games for collecting transition data to

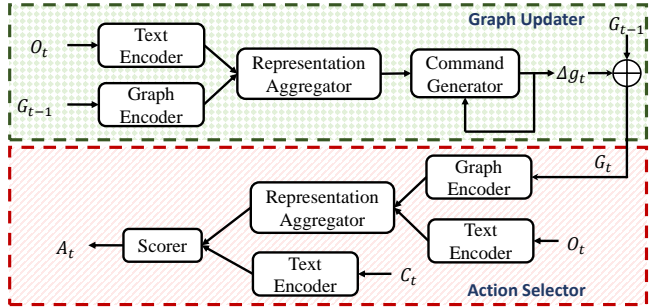


Figure 2. GATA in detail. The coloring scheme is same as in Figure 1. The graph updater first generates  $\Delta g_t$  using  $\mathcal{G}_{t-1}$  and  $O_t$ . Afterwards the action selector uses  $O_t$  and the updated graph  $\mathcal{G}_t$  to select  $\mathcal{A}_t$  from the list of action candidates  $C_t$ .

pre-train our model’s graph updater (Section 4.3) and graph encoder (Section 4.2). Note that there is no overlap between the *FTWP* games and the games we use in Section 5.

## 3. Graph Aided Transformer Agent (GATA)

In this section, we introduce GATA, a novel transformer-based neural agent that can leverage both text and KGs as input modalities. As shown in Figure 2, the agent consists of two main modules: a graph updater and an action selector. At game step  $t$ , the graph updater extracts relevant information from raw text  $O_t$  and updates its belief graph  $\mathcal{G}_t^{\text{belief}}$  accordingly. The action selector issues action  $\mathcal{A}_t$  conditioned on  $O_t$  and the KG provided to it (either  $\mathcal{G}_t^{\text{full}}$ ,  $\mathcal{G}_t^{\text{seen}}$ , or  $\mathcal{G}_t^{\text{belief}}$ ). Note that the graph updater is only active in the case that we use  $\mathcal{G}_t^{\text{belief}}$  as the KG. Figure 1 illustrates the interaction between GATA and a game in this case.

### 3.1. Action Selector

As shown in Figure 2, the action selector consists of four main components: the text encoder and graph encoder convert text inputs and graph inputs respectively into hidden representations; a representation aggregator fuses the two representations using an attention mechanism; and a scorer provides a ranking for all candidate actions as output. In some experimental settings, the text observation  $O_t$  can be absent. In these cases, the representation aggregator is disabled and the output of the graph encoder is fed directly into the scorer.

**Graph Encoder:** Since graphs in text-based games are multi-relational (see Figure 1), we use relational graph convolutional networks (R-GCNs) (Schlichtkrull et al., 2018) to capture representations of the multi-relational KGs that model the game states. A standard R-GCN does not consider semantic information contained in the relation labels. In our task, however, relation labels may contain useful informa-

tion (e.g., `east_of` and `west_of` are reciprocal relations). Therefore, we learn a vector representation for each relation conditioned on the text label’s word embeddings. We use the concatenation of the resulting vector with the node embeddings as the input to each R-GCN layer (an ablation study for relation embeddings is provided in Appendix B.5). Additionally, our R-GCN uses basis regularization (Schlichtkrull et al., 2018) and highway connections (Srivastava et al., 2015) between layers for faster convergence. Details are provided in Appendix A.1.

**Text Encoder:** Transformer models (Vaswani et al., 2017) achieve strong performance on a host of NLP tasks (Devlin et al., 2018; Yu et al., 2018). We adopt a transformer-based encoder to convert text inputs into contextual vector representations. Details are provided in Appendix A.2.

**Representation Aggregator:** We use a bi-directional attention-based aggregator (Yu et al., 2018; Seo et al., 2016) to combine text and graph representations. Attention from text to graph enables the agent to focus more on nodes that appear in text observations, which are generally more relevant at the given time step; attention from nodes to text enables the agent to focus more on text representations where the underlying tokens are in the KG, and therefore connected with the player in certain relations. Details are provided in Appendix A.3.

**Scorer:** The scorer consists of a self-attention layer and a multi-layer perceptron (MLP). First, the self-attention layer reinforces the dependency of every token-token pair and node-node pair in the aggregated representations. The resulting vectors are concatenated with the representations of action candidates  $C_t$  (from the text encoder). The MLP then uses the concatenated vectors to generate a single scalar for every action candidate. These are used to select the best action. Details are provided in Appendix A.4.

### 3.2. Graph Updater

The graph updater constructs and updates a dynamic knowledge graph (i.e.,  $\mathcal{G}^{\text{belief}}$ ) using text observations, so that GATA can leverage structured information even when ground-truth KGs are unavailable (the most realistic case). Rather than generating the entire belief graph at every game step  $t$ , we generate a set of update operations  $\Delta g_t$  that represent the change of the belief graph:

$$\mathcal{G}_t^{\text{belief}} = \mathcal{G}_{t-1}^{\text{belief}} \oplus \Delta g_t, \quad (1)$$

where  $\oplus$  is a set operation function that applies  $\Delta g_t$ . In this work, we use discrete update operations that act on the explicit KG (as opposed to, say, real-valued vector updates to a KG encoding). In particular, we model each update operation in  $\Delta g_t$  as a sequence of tokens. We define the following two elementary operations so that any graph

---

```

add (player, shed, at)
add (shed, backyard, west_of)
add (wooden door, shed, east_of)
add (toolbox, shed, in)
add (toolbox, closed, is)
add (workbench, shed, in)
delete (player, backyard, at)

```

---

Table 1. Update operations matching the transition in Figure 1.

update can be achieved in  $k \geq 0$  such operations:

- `add(node1, node2, relation)`: add a directed edge, named `relation`, between `node1` and `node2`.
- `delete(node1, node2, relation)`: delete a directed edge, named `relation`, between `node1` and `node2`.

Given a new observation string  $O_t$  and  $\mathcal{G}_{t-1}^{\text{belief}}$ , the agent generates  $k \geq 0$  such operations to merge the newly observed information into its belief graph. For the example shown in Figure 1, the generated operations are listed in Table 1.

We formulate the update generation task as a sequence-to-sequence (Seq2Seq) problem and use a transformer-based model (Vaswani et al., 2017) to generate token sequences for the operations. The Seq2Seq model uses an encoder structure similar to that of the action selector described in Section 3.1 (see Figure 2). At the command generator layer, we use a standard transformer decoder to generate update operations (details are provided in Appendix A.5). We adopt the decoding strategy from (Meng et al., 2019), where given an observation sequence  $O_t$  and a belief graph  $\mathcal{G}_{t-1}^{\text{belief}}$ , the agent generates a sequence of tokens that contains multiple graph update operations as subsequences, separated by a delimiter token. Since Seq2Seq set generation models are known to learn better with a consistent output ordering (Meng et al., 2019), we sort the ground-truth operations (e.g., always `add` before `delete`) for training.

## 4. Training GATA

We train different components of GATA with different strategies. For the action selector, we train with reinforcement learning based on reward signals from the set of training games. We use supervised teacher forcing to pre-train the graph updater and keep it frozen while the action selector interacts with the environment. We use a similar approach for the graph encoder, exploring several graph-based pre-training tasks.

### 4.1. Training the Action Selector

We use Q-learning (Watkins & Dayan, 1992) to optimize the action selector on reward signals from training games. Specifically, we use Double DQN (van Hasselt et al., 2015) combined with multi-step learning (Sutton, 1988) and pri-

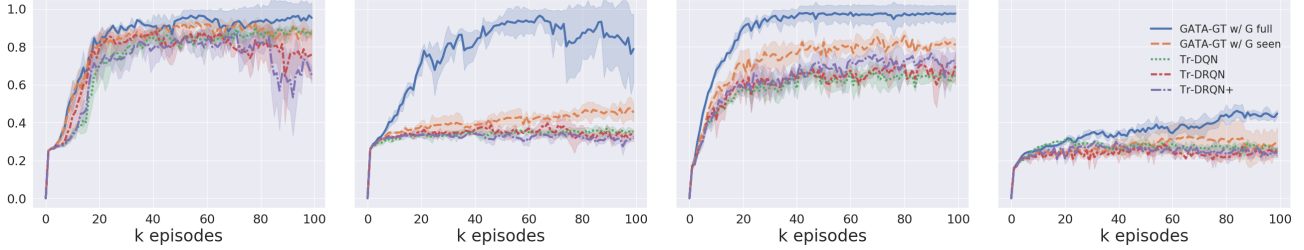


Figure 3. Training curves (averaged over 3 seeds, band represents standard deviation) on 20 games for difficulty level 1/2/3/4. The y-axis denote the normalized rewards i.e. score achieved/max possible score.

---

**Algorithm 1** Training Strategy for GATA
 

---

```

1: Input: games  $\mathcal{X}$ , replay buffer  $B$ , update frequency  $F$ , patience  $P$ , tolerance  $\tau$ , evaluation frequency  $E$ .
2: Initialize counters  $k \leftarrow 1, p \leftarrow 0$ , best validation score  $V \leftarrow 0$ , transition cache  $C$ , policy  $\pi$ , checkpoint  $\Pi$ .
3: for  $e \leftarrow 1$  to NB.EPISODES do
4:   Sample a game  $x \in \mathcal{X}$ , reset  $C$ .
5:   for  $i \leftarrow 1$  to NB.STEPS do
6:     play game, push transition into  $C$ ,  $k \leftarrow k + 1$ 
7:     if  $k\%F = 0$  then sample batch from  $B$ , Update( $\pi$ )
8:     if done then break
9:   end for
10:  if average score in  $C > \tau \cdot$  average score in  $B$  then
11:    for all item in  $C$  do push item into  $B$ 
12:  end if
13:  if  $e\%E \neq 0$  then continue
14:   $v \leftarrow$  Evaluate( $\pi$ )
15:  if  $v \geq V$  then  $\Pi \leftarrow \pi, p \leftarrow 0$ , continue
16:  if  $p > P$  then  $\pi \leftarrow \Pi, p \leftarrow 0$ 
17:  else  $p \leftarrow p + 1$ 
18: end for
    
```

---

ortized experience replay (Schaul et al., 2016). To enable GATA to scale and generalize to multiple games, we adapt standard deep Q-Learning by sampling a new game  $x$  from the set of training games  $\mathcal{X}$  to collect an episode (see Algorithm 1, line 4), meaning that the replay buffer  $B$  contains transitions from episodes on different games.

Additionally, we report two strategies that we empirically find effective in DQN training. First, we discard the under-achieving trajectories without pushing them into the replay buffer (lines 10–12). Specifically, we only push a new trajectory that has an average reward greater than  $\tau \in \mathbb{R}_0^+$  times the average reward for all transitions in the replay buffer. We use  $\tau = 0.1$ , since it keeps around some weaker but acceptable trajectories and does not limit exploration too severely. Second, we keep track of the best performing policy  $\Pi$  on the validation games. During training, when GATA stops improving on validation games, we load  $\Pi$  back to the training policy  $\pi$  and resume training. After training, we report the performance of  $\Pi$  on test games. The overall training procedure is shown in Algorithm 1. Note these two strategies are not designed specifically for GATA; rather, we

find them effective in DQN training in general.

Although we have a graph updater that can construct  $\mathcal{G}_t^{\text{belief}}$ , we always use ground-truth KGs while training the action selector. This prevents the accumulation of errors from the graph updater, which would make the RL training unstable. Thus,  $\mathcal{G}_t^{\text{belief}}$  is input to the selector only during evaluation.

## 4.2. Pre-training the Graph Encoder

We explore several self-supervised and supervised learning tasks for pre-training the action selector’s graph encoder, since we consider it too difficult to learn effective encodings from reward signals alone. The pre-training methods we introduce help the graph encoder to capture effective graph embeddings and to understand generic dynamics of the games. For this purpose we use transitions collected from the *FTWP* dataset (as described in Section 2.2). We keep the original split of training, validation, and test sets, with difficulty levels mixed together, and use them to generate training, validation, and test sets for each of our pre-training tasks. We propose four tasks, including three classification tasks and one generation task, that are briefly described below (refer to Appendix B for details) :

**Action Prediction (AP):** Given  $\mathcal{G}_{t-1}$  and  $\mathcal{G}_t$ , an agent is required to select  $\mathcal{A}_{t-1}$  from a set of candidate actions with negative samples in it. This task trains a model to capture the *inverse* dynamics of the environment, since it estimates the action that *causes* the state transition  $\mathcal{S}_{t-1} \rightarrow \mathcal{S}_t$ . This is inspired by the work of Pathak et al. (2017); Agrawal et al. (2016), which shows that estimating the inverse model dynamics greatly aids multi-step decision making for vision-based RL.

**State Prediction (SP):** Given  $\mathcal{G}_{t-1}$  and  $\mathcal{A}_{t-1}$ , an agent is required to select  $\mathcal{G}_t$  from a set of candidate graphs with negative samples in it. Compared to the AP task, SP trains a model to capture the *forward* dynamics of the environments since it estimates the *effect* of an action  $\mathcal{A}_{t-1}$  conditioned on the previous state  $\mathcal{S}_{t-1}$ .

**Deep Graph Infomax (DGI):** Contrary to AP and SP, which model the dynamics of the environment, the DGI

Level	#I	#R	S	Cut	Cook	#C	#N	D
1	1	1	4	✓	✗	8.9	17.1	0.013
2	1	1	5	✓	✓	8.9	17.5	0.013
3	1	9	3	✗	✗	4.9	34.1	0.004
4	3	6	11	✓	✓	10.8	33.4	0.005

Table 2. Statistics of games. #I: number of ingredients in a recipe; #R: number of locations in a game; S: the max score an agent can achieve; #C: the average number of action candidates at a step; #N: averaged number of nodes per game; D: averaged edge density.

task (Veličković et al., 2019) enables a model to learn graph representations at the node level. The graph encoder is trained to distinguish true node representations of a graph  $\mathcal{G}$  from corrupted representations.

**Command Generation (CG):** We consider the task of generating graph update operations (described in Section 3.2) as an alternative graph representation learning method. A detailed overview of this task is provided in Section 4.3.

### 4.3. Training the Graph Updater

The graph updater is also trained on the collection of transitions from *FTWP*. Although it can be trained on-the-fly while interacting with a game, we find pre-training more effective, since we can easily leverage a more diverse set of transitions. For every transition that contains two consecutive graphs, we convert the difference between the graphs to ground-truth update operations (examples provided in Table 1). We use teacher forcing to train the entire Seq2Seq graph updater by optimizing the negative log-likelihood loss. During training, a right-shifted ground-truth update operation is provided as input to the decoder. Once trained in this manner, the graph updater parameters are frozen.

The graph updater provides  $\mathcal{G}_t^{\text{belief}}$  to the action selector at every game step as GATA interacts with the game, but is not trained further during this interaction in this work. At every game step, the graph updater generates commands token-by-token until it generates an end-of-sequence token or it hits the maximum sequence length limit. Note that despite sharing similar structures, by default, no parameters are shared between the action selector and graph updater. Further details on training and validating the graph updater are provided in Appendix D.

## 5. Experiments and Analysis

In this work we conduct experiments on cooking themed text-based games (as described in Section 2.2) that we generate using TextWorld (Côté et al., 2018). We divide the games into four subsets with one difficulty level per subset. Each subset contains 100 training games, 20 validation games, and 20 test games, which are sampled from a distribution that is determined by their difficulty level. For easier

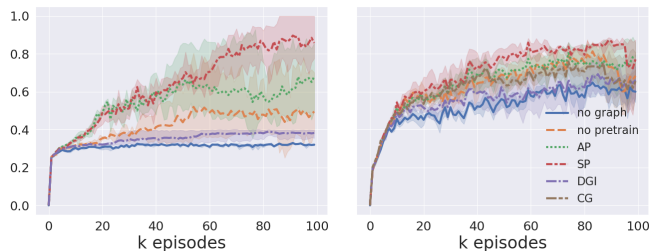


Figure 4. Training curves (averaged over 3 seeds, band represents standard deviation) on 100 games for difficulty level 2 (left) and 3 (right). Color indicates different pre-training methods. The y-axis denotes normalized score. From left to right, inputs to the agent are  $\mathcal{G}^{\text{full}}$  and  $\mathcal{G}^{\text{seen}}$ , respectively.

games, the recipe might only require a single ingredient, and the world is limited to a single location, whereas harder games might have a recipe requiring up to three ingredients randomly distributed across 6 locations. We provide the statistics of the games in Table 2.

As baselines, we use our implementation of LSTM-DQN (Narasimhan et al., 2015) and LSTM-DRQN (Yuan et al., 2018), both of which use only  $O_t$  as input. Note that LSTM-DRQN enables some generalization by using a recurrent neural network to condition its decisions on its memory (i.e., belief), and an episodic counting bonus to encourage exploration. This draws an interesting comparison with GATA, wherein the belief is extracted and updated dynamically, in the form of a KG. For fair comparison, we replace the LSTM-based text encoder of both LSTM-DQN and LSTM-DRQN with a transformer-based text encoder as in GATA. We denote those agents as Tr-DQN and Tr-DRQN respectively. We denote a Tr-DRQN equipped with the episodic counting bonus as Tr-DRQN+. These three text-based baselines are representative of the current top-performing neural agents on text-based games. We denote our agent that maintains and updates its belief graph ( $\mathcal{G}^{\text{belief}}$ ) using text observation as GATA, and the version that uses ground-truth graphs ( $\mathcal{G}^{\text{full}}$  or  $\mathcal{G}^{\text{seen}}$ ) as GATA-GT. The pre-trained graph updater we use achieves **0.968** test  $F_1$  score on the dataset described in Section 4.3. We vary our experiments along three settings and use them to answer different questions about playing text-based games with KGs.

### Proof-of-Concept: Graph Input vs. Text Input?

Most previous text-based game literature focuses on training with a single game because it remains challenging to optimize an RL agent on a distribution of environments. One of our main hypotheses is that structured KG input, compared to text input only, can help an RL agent to achieve better performance when trained on *multiple* games and to generalize better to unseen games. To verify that hypothesis, we first

## Learning Dynamic Knowledge Graphs to Generalize on Text-based Games

		20 Training Games					100 Training Games					Avg.
Difficulty Level		1	2	3	4	% ↑	1	2	3	4	% ↑	% ↑
Input	Agent	Text as Input ( $\mathcal{G}_t^{\text{belief}}$ is generated by GATA)										
$O_t$	Tr-DQN	<b>66.2</b>	26.0	16.7	<b>18.2</b>	—	<b>62.5</b>	32.0	38.3	17.7	—	—
$O_t$	Tr-DRQN	62.5	<b>32.0</b>	28.3	12.7	+14.2	58.8	31.0	36.7	21.4	+1.9	+8.1
$O_t$	Tr-DRQN+	65.0	30.0	35.0	11.8	+22.0	58.8	<b>33.0</b>	33.3	19.5	-1.4	+10.3
$\mathcal{G}_t^{\text{belief}}$	GATA	65.0	24.0	33.3	15.9	+19.3	<b>62.5</b>	30.0	45.0	<b>26.4</b>	<b>+15.1</b>	+17.2
$\mathcal{G}_t^{\text{belief}}$ and $O_t$	GATA	58.8	<b>32.0</b>	<b>38.3</b>	16.8	<b>+33.4</b>	<b>62.5</b>	32.0	<b>48.3</b>	20.0	+9.8	<b>+21.6</b>
Ground-truth Seen Graphs as Input												
$\mathcal{G}_t^{\text{seen}}$	GATA-GT	60.0	34.0	30.0	19.1	+26.5	58.8	33.0	43.3	30.9	+21.2	+23.9
Ground-truth Full Graphs as Input												
$\mathcal{G}_t^{\text{full}}$	GATA-GT	48.7	61.0	46.7	23.6	+79.4	95.0	95.0	70.0	37.3	+110.6	+95.0

Table 3. Agents’ normalized **test** scores and averaged relative improvement (% ↑) over Tr-DQN across difficulty levels. An agent  $m$ ’s relative improvement over Tr-DQN is defined as  $(R_m - R_{\text{Tr-DQN}})/R_{\text{Tr-DQN}}$  where  $R$  is the score. All numbers are percentages.

analyze the training performance of GATA-GT compared against the three text-based baselines. Note that we do not extract and update  $\mathcal{G}^{\text{belief}}$  when training the action selector (as described in Section 4.1).  $\mathcal{G}^{\text{belief}}$  is used only during testing. Figure 3 shows the agents’ performance when training on 20 games for each difficulty level. We observe a clear trend where agents with graph input consistently outperform the agents without (consistent when training on 100 games as well). These results provide evidence that an RL agent can achieve better training scores and learn faster with structured input. Since the ground-truth graphs contain the full information a graph-based agent could obtain, the performance of GATA-GT sets an approximate but reasonable upper-bound for GATA (since a perfect graph updater will yield  $\mathcal{G}^{\text{belief}} = \mathcal{G}^{\text{seen}}$ ). In the following subsections, we show GATA can achieve better generalization performance than text-only agents even when ground-truth graphs are unavailable.

### 5.1. Can Agents Generalize to Unseen Games?

Once trained, we report agents’ performance on test games. To fairly compare with Tr-DQN, Tr-DRQN and Tr-DRQN+, GATA in this set of experiments takes only text observations as input and dynamically updates its belief graph using the graph updater described in Section 3.2. Again, we also provide GATA-GT’s performance as an upper-bound to GATA.

In Table 3, we show the normalized rewards on test games achieved by agents trained on either 20 or 100 games for each difficulty level. We tune hyperparameters on the validation games, selecting the top-performing agent for each model (see Appendix D for details). In the table, % ↑ denotes the averaged relative improvement of an agent over

Tr-DQN. We can observe that Tr-DRQN and Tr-DRQN+ outperform Tr-DQN, with 8.1% and 10.3% relative improvement, respectively. This suggests the implicit memory mechanism of recurrent components helps in generalizing across games, as expected. GATA outperforms Tr-DQN by 17.2% with  $\mathcal{G}^{\text{belief}}$  maintained by itself. When combining  $\mathcal{G}^{\text{belief}}$  with the text observations used to update it, GATA gets an average relative improvement of 21.6% over Tr-DQN. The gap between the two scores obtained by GATA suggests that the updated belief graphs are not always perfect, since the potentially more accurate text observations are useful.

It is not surprising that GATA-GT performs much better when ground-truth graphs are available, especially with  $\mathcal{G}^{\text{full}}$ , which makes the games fully-observable. However, it is interesting to see that GATA with the belief graph can achieve performance close to its upper-bound (the model with  $\mathcal{G}^{\text{seen}}$  as input). We also observe that agents trained on 100 games generalize better than those trained on 20 games. This is not unexpected, but emphasizes the importance of training agents on a distribution of games rather than a single game.

From this set of experiments we conclude that KGs enable agents to train on multiple games more effectively, while agents trained on more games generalize better. In this sense, KGs help agents generalize on text-based games.

### 5.2. Do Pre-trained Graph Encoders Help?

We show in previous subsections that KGs help training with multiple games and generalizing to unseen games. In this subsection, we explore to what extent pre-training the graph encoder is beneficial. We provide detailed pre-training results in Appendix B.5.

Difficulty Level	1	2	3	4	% $\uparrow$
Tr-DQN	62.5	32.0	38.3	17.7	—
Tr-DRQN	58.8	31.0	36.7	21.4	+1.9
Tr-DRQN+	58.8	<b>33.0</b>	33.3	19.5	-1.4
Pre-train	GATA				
N/A	62.5	30.0	45.0	26.4	+15.1
AP	66.2	25.0	<b>50.0</b>	<b>29.5</b>	<b>+20.3</b>
SP	58.8	<b>33.0</b>	45.0	28.6	+19.1
DGI	<b>70.0</b>	30.0	43.3	20.0	+7.9
CG	66.2	32.0	40.0	16.4	+0.8

Table 4. Agents’ test scores and averaged relative improvement over Tr-DQN. Agent trained on 100 games. At game step  $t$ , GATA updates  $\mathcal{G}_t^{\text{belief}}$  and use as input. Shading represents numbers that are greater than or equal to all the text-based baselines.

Figure 4 shows training curves of GATA-GT when the graph encoder is initialized using the different pre-training tasks described in Section 4.2. For comparison, we provide training curves for Tr-DQN and a GATA-GT with randomly initialized graph encoders. Test scores for GATA are given in Table 4, where we compare variants pre-trained with the different tasks. From Figure 4 and Table 4, we observe that the AP and SP tasks generally help the most, whereas DGI and CG do not show a significant effect. The lack of gains from DGI and CG highlight the importance of using pre-training tasks that incorporate both graph structure and game dynamics (i.e., how actions affect the graphs across time steps).

### 5.3. Additional Results

Due to space limitations, we only report the most representative segment of our results in this section. In Appendix C we provide an exhaustive results set that includes GATA-GT’s training curves, training scores, test scores, and GATA’s test scores across all difficulties and pre-training settings. We also relate some additional observations we made in our attempts to solve text-based games with GATA and provide possible explanations (e.g. in what conditions does DGI work better, or why does GATA-GT with  $\mathcal{G}_t^{\text{full}}$  perform poorly on level 1 games?). We strongly encourage readers to see the full results of our experiments.

## 6. Related Work

### 6.1. Dynamic KG extraction

There have been numerous recent works focused on constructing KGs to encode structured representations from raw data for various tasks. Kipf et al. (2020) propose contrastive methods to learn latent structured world models (C-SWMs) as state representations for vision-based environments. That work, however, does not focus on learn-

ing policies to play games or to generalize across varying environments. Das et al. (2018) leverage a machine reading comprehension (MRC) mechanism to query for entities and states in short text passages and use a dynamic graph structure to track changing entity states. Fan et al. (2019) propose to construct local graph-structured knowledge bases in query-based open-domain NLP tasks, and to encode the graph representations by linearizing the graph into a structured input sequence. Johnson (2016) achieve good performance on the bAbI tasks (Weston et al., 2015) by constructing graphs from text data using gated graph transformer neural networks. Yang et al. (2018) learn transferrable generic latent relational graphs from raw data in an unsupervised manner. Compared to the above literature, in this work we aim to dynamically extract multi-relational KGs from partial text observations of the state, which can inform general policies.

### 6.2. Playing Text-based Games

Recent years have seen a host of work on and around playing text-based games. Various deep learning agents have been explored to play text-based games (Narasimhan et al., 2015; He et al., 2015; Hausknecht et al., 2019a; Zahavy et al., 2018; Jain et al., 2019; Ammanabrolu & Hausknecht, 2020; Zelinka, 2018; Yin & May, 2019a). Fulda et al. (2017) use pre-trained embeddings to reduce the action space. Zahavy et al. (2018), Seurin et al. (2019) and Jain et al. (2019) propose to explicitly condition an agent’s decisions on game feedback. Most of this literature trains and tests on the same single game, without considering generalization.

Urbanek et al. (2019) use memory networks and ranking systems to tackle adventure-themed dialog tasks. Yuan et al. (2018) propose a count-based memory to explore and generalize to simple unseen text-based games. Madotto et al. (2020) use GoExplore (Ecoffet et al., 2019) with imitation learning to generalize. Adolphs & Hofmann (2019) and Yin & May (2019b) also investigate the multi-game setting. However, those methods rely either on reward shaping by heuristics, imitation learning, or rule-based features as inputs. We aim to minimize hand-crafting, so our action selector is optimized only using raw rewards from games and other components of our model are pretrained on related data. Recently Ammanabrolu & Riedl (2018); Ammanabrolu & Hausknecht (2020); Yin & May (2019b) propose to leverage a KG to play text-based games using rule-based, untrained mechanisms to construct the KGs for a deep learning system.

## 7. Conclusion

In this work, we investigated how KGs can facilitate an RL agent’s learning and zero-shot generalization in text-based games. We introduce GATA, a novel neural agent

that builds and leverage KGs to achieve better training and test performance compared to baseline text-based agents. GATA is able to construct and update its “belief” state as a KG, which is further used to achieve better generalization when ground-truth KGs are unavailable. We investigated four graph representation learning tasks to pre-train GATA, and we show they can further improve training and test performance on unseen games.

## References

- Adolphs, L. and Hofmann, T. Ledeechef: Deep reinforcement learning agent for families of text-based games. *CoRR*, abs/1909.01646, 2019. URL <https://arxiv.org/abs/1909.01646>.
- Agrawal, P., Nair, A. V., Abbeel, P., Malik, J., and Levine, S. Learning to poke by poking: Experiential learning of intuitive physics. In Lee, D. D., Sugiyama, M., Luxburg, U. V., Guyon, I., and Garnett, R. (eds.), *Advances in Neural Information Processing Systems 29*, pp. 5074–5082. Curran Associates, Inc., 2016.
- Ammanabrolu, P. and Hausknecht, M. Graph constrained reinforcement learning for natural language action spaces. In *International Conference on Learning Representations*, 2020. URL <https://openreview.net/forum?id=B1x6w0EtWH>.
- Ammanabrolu, P. and Riedl, M. O. Playing text-adventure games with graph-based deep reinforcement learning. *CoRR*, abs/1812.01628, 2018. URL <http://arxiv.org/abs/1812.01628>.
- Atkinson, T., Baier, H., Coppelstone, T., Devlin, S., and Swan, J. The text-based adventure ai competition. *IEEE Transactions on Games*, 11:260–266, 2018.
- Ba, L. J., Kiros, J. R., and Hinton, G. E. Layer normalization. *CoRR*, abs/1607.06450, 2016. URL <http://arxiv.org/abs/1607.06450>.
- Côté, M.-A., Kádár, A., Yuan, X., Kybartas, B., Barnes, T., Fine, E., Moore, J., Tao, R. Y., Hausknecht, M., Asri, L. E., Adada, M., Tay, W., and Trischler, A. Textworld: A learning environment for text-based games. *CoRR*, abs/1806.11532, 2018.
- Das, R., Munkhdalai, T., Yuan, X., Trischler, A., and McCallum, A. Building dynamic knowledge graphs from text using machine reading comprehension. *CoRR*, abs/1810.05682, 2018. URL <http://arxiv.org/abs/1810.05682>.
- Devlin, J., Chang, M., Lee, K., and Toutanova, K. BERT: pre-training of deep bidirectional transformers for language understanding. *CoRR*, abs/1810.04805, 2018. URL <http://arxiv.org/abs/1810.04805>.
- Ecoffet, A., Huizinga, J., Lehman, J., Stanley, K. O., and Clune, J. Go-explore: a new approach for hard-exploration problems. *ArXiv*, abs/1901.10995, 2019.
- Fan, A., Gardent, C., Braud, C., and Bordes, A. Using local knowledge graph construction to scale seq2seq models to multi-document inputs. *CoRR*, abs/1910.08435, 2019. URL <https://arxiv.org/abs/1910.08435>.
- Fulda, N., Ricks, D., Murdoch, B., and Wingate, D. What can you do with a rock? affordance extraction via word embeddings. *CoRR*, abs/1703.03429, 2017. URL <http://arxiv.org/abs/1703.03429>.
- Hausknecht, M., Ammanabrolu, P., Marc-Alexandre, C., and Xingdi, Y. Interactive fiction games: A colossal adventure. *CoRR*, abs/1909.05398, 2019a. URL <http://arxiv.org/abs/1909.05398>.
- Hausknecht, M. J., Loynd, R., Yang, G., Swaminathan, A., and Williams, J. D. NAIL: A general interactive fiction agent. *CoRR*, abs/1902.04259, 2019b. URL <http://arxiv.org/abs/1902.04259>.
- He, J., Chen, J., He, X., Gao, J., Li, L., Deng, L., and Ostendorf, M. Deep reinforcement learning with an unbounded action space. *CoRR*, abs/1511.04636, 2015. URL <http://arxiv.org/abs/1511.04636>.
- Hessel, M., Modayil, J., van Hasselt, H., Schaul, T., Ostrovski, G., Dabney, W., Horgan, D., Piot, B., Azar, M. G., and Silver, D. Rainbow: Combining improvements in deep reinforcement learning. *CoRR*, abs/1710.02298, 2017.
- Jain, V., Fedus, W., Larochelle, H., Precup, D., and Belle-mare, M. G. Algorithmic improvements for deep reinforcement learning applied to interactive fiction. *CoRR*, abs/1911.12511, 2019. URL <https://arxiv.org/abs/1911.12511>.
- Johnson, D. D. Learning graphical state transitions. 2016. URL <https://openreview.net/pdf?id=HJ0NvFzxl>.
- Kipf, T., van der Pol, E., and Welling, M. Contrastive learning of structured world models. In *International Conference on Learning Representations*, 2020. URL <https://openreview.net/forum?id=H1gax6VtDB>.
- Lima, P. Cognitextworldagent, 2019. URL <https://github.com/pvl/CogniTextWorldAgent>.
- Liu, L., Jiang, H., He, P., Chen, W., Liu, X., Gao, J., and Han, J. On the variance of the adaptive learning rate and beyond. *arXiv preprint arXiv:1908.03265*, 2019.

- Madotto, A., Namazifar, M., Huizinga, J., Molino, P., Ecoffet, A., Zheng, H., Papangelis, A., Yu, D., Khatri, C., and Tur, G. Exploration based language learning for text-based games, 2020. URL <https://openreview.net/forum?id=BygSXCNFDB>.
- Meng, R., Yuan, X., Wang, T., Brusilovsky, P., Trischler, A., and He, D. Does order matter? an empirical study on generating multiple keyphrases as a sequence. *CoRR*, 2019.
- Mikolov, T., Grave, E., Bojanowski, P., Puhersch, C., and Joulin, A. Advances in pre-training distributed word representations. In *Proceedings of the International Conference on Language Resources and Evaluation (LREC 2018)*, 2018.
- Narasimhan, K., Kulkarni, T., and Barzilay, R. Language understanding for text-based games using deep reinforcement learning. In *Proceedings of the 2015 Conference on Empirical Methods in Natural Language Processing*, pp. 1–11, Lisbon, Portugal, September 2015. Association for Computational Linguistics. doi: 10.18653/v1/D15-1001. URL <https://www.aclweb.org/anthology/D15-1001>.
- Paszke, A., Gross, S., Chintala, S., Chanan, G., Yang, E., DeVito, Z., Lin, Z., Desmaison, A., Antiga, L., and Lerer, A. Automatic differentiation in pytorch. In *NIPS-W*, 2017.
- Pathak, D., Agrawal, P., Efros, A. A., and Darrell, T. Curiosity-driven exploration by self-supervised prediction. In *ICML*, 2017.
- Schaul, T., Quan, J., Antonoglou, I., and Silver, D. Prioritized experience replay. In *International Conference on Learning Representations*, Puerto Rico, 2016.
- Schlichtkrull, M., Kipf, T. N., Bloem, P., Van Den Berg, R., Titov, I., and Welling, M. Modeling relational data with graph convolutional networks. In *European Semantic Web Conference*, pp. 593–607. Springer, 2018.
- Seo, M., Kembhavi, A., Farhadi, A., and Hajishirzi, H. Bidirectional attention flow for machine comprehension. *arXiv preprint arXiv:1611.01603*, 2016.
- Seurin, M., Preux, P., and Pietquin, O. “i’m sorry dave, i’m afraid i can’t do that” deep q-learning from forbidden action. *CoRR*, abs/1910.02078, 2019. URL <https://arxiv.org/abs/1910.02078>.
- Srivastava, R. K., Greff, K., and Schmidhuber, J. Highway networks. *CoRR*, abs/1505.00387, 2015. URL <http://arxiv.org/abs/1505.00387>.
- Sutton, R. *The Bitter Lesson*, 2019. URL <http://www.incompleteideas.net/IncIdeas/BitterLesson.html>.
- Sutton, R. S. Learning to predict by the methods of temporal differences. *Machine Learning*, 3(1):9–44, Aug 1988. ISSN 1573-0565. doi: 10.1007/BF00115009. URL <https://doi.org/10.1007/BF00115009>.
- Trischler, A., Côté, M.-A., and Lima, P. *First TextWorld Problems, the competition: Using text-based games to advance capabilities of AI agents*, 2019. URL <https://aka.ms/ftwp-msr-blog-post>.
- Urbanek, J., Fan, A., Karamcheti, S., Jain, S., Humeau, S., Dinan, E., Rocktäschel, T., Kiela, D., Szlam, A., and Weston, J. Learning to speak and act in a fantasy text adventure game. *CoRR*, abs/1903.03094, 2019. URL <http://arxiv.org/abs/1903.03094>.
- van Hasselt, H., Guez, A., and Silver, D. Deep reinforcement learning with double q-learning. In *AAAI*, 2015.
- Vaswani, A., Shazeer, N., Parmar, N., Uszkoreit, J., Jones, L., Gomez, A. N., Kaiser, L. u., and Polosukhin, I. Attention is all you need. In Guyon, I., Luxburg, U. V., Bengio, S., Wallach, H., Fergus, R., Vishwanathan, S., and Garnett, R. (eds.), *Advances in Neural Information Processing Systems 30*, pp. 5998–6008. Curran Associates, Inc., 2017. URL <http://papers.nips.cc/paper/7181-attention-is-all-you-need.pdf>.
- Veličković, P., Fedus, W., Hamilton, W. L., Liò, P., Bengio, Y., and Hjelm, R. D. Deep Graph Infomax. In *International Conference on Learning Representations*, 2019. URL <https://openreview.net/forum?id=rklz9iAcKQ>.
- Watkins, C. J. C. H. and Dayan, P. Q-learning. *Machine Learning*, 8(3):279–292, May 1992. ISSN 1573-0565. doi: 10.1007/BF00992698. URL <https://doi.org/10.1007/BF00992698>.
- Weston, J., Bordes, A., Chopra, S., and Mikolov, T. Towards ai-complete question answering: A set of prerequisite toy tasks. *CoRR*, abs/1502.05698, 2015.
- Yang, Z., Zhao, J. J., Dhingra, B., He, K., Cohen, W. W., Salakhutdinov, R., and LeCun, Y. Glomo: Unsupervisedly learned relational graphs as transferable representations. *ArXiv*, abs/1806.05662, 2018.
- Yin, X. and May, J. Comprehensible context-driven text game playing. *CoRR*, abs/1905.02265, 2019a. URL <http://arxiv.org/abs/1905.02265>.

- Yin, X. and May, J. Learn how to cook a new recipe in a new house: Using map familiarization, curriculum learning, and bandit feedback to learn families of text-based adventure games. *CoRR*, abs/1908.04777, 2019b. URL <https://arxiv.org/abs/1908.04777>.
- Yu, A. W., Dohan, D., Luong, M., Zhao, R., Chen, K., Norouzi, M., and Le, Q. V. Qanet: Combining local convolution with global self-attention for reading comprehension. *CoRR*, abs/1804.09541, 2018. URL <http://arxiv.org/abs/1804.09541>.
- Yuan, X., Côté, M.-A., Sordani, A., Laroche, R., Combes, R. T. d., Hausknecht, M., and Trischler, A. Counting to explore and generalize in text-based games. *arXiv preprint arXiv:1806.11525*, 2018.
- Zahavy, T., Haroush, M., Merlis, N., Mankowitz, D. J., and Mannor, S. Learn what not to learn: Action elimination with deep reinforcement learning. *CoRR*, abs/1809.02121, 2018. URL <http://arxiv.org/abs/1809.02121>.
- Zelinka, M. Baselines for reinforcement learning in text games. *2018 IEEE 30th International Conference on Tools with Artificial Intelligence (ICTAI)*, pp. 320–327, 2018.

## A. Details of GATA

### Notations

In this section, we use  $o_t$  to denote text observation at game step  $t$ ,  $C_t$  to denote a list of action candidate provided by a game, and  $\mathcal{G}_t$  to denote a KG that represents the state. Note  $\mathcal{G}_t$  can either be fully observable ( $\mathcal{G}_t^{\text{full}}$ ), partially observable ( $\mathcal{G}_t^{\text{seen}}$ ), or constructed and updated by the the graph updater ( $\mathcal{G}_t^{\text{belief}}$ ).

We use  $L$  to refer to a linear transformation and  $L^f$  means it is followed by a non-linear activation function  $f$ . Brackets  $[\cdot; \cdot]$  denote vector concatenation. Overall structure of GATA is shown in Figure 2.

### A.1. Graph Encoder

As briefly mentioned in Section 3.1, GATA utilizes a graph encoder which is based on R-GCN (Schlichtkrull et al., 2018).

To better leverage information from relation labels, when computing each node’s representation, we also condition it on a relation representation  $E$ :

$$h_i^l = \sigma \left( \sum_{r \in \mathcal{R}} \sum_{j \in \mathcal{N}_i^r} W_r^l [h_j^l; E_r] + W_0^l [h_i^l; E_r] \right), \quad (2)$$

in which,  $l$  denotes the  $l$ -th layer of the R-GCN,  $\mathcal{N}_i^r$  denotes the set of neighbor indices of node  $i$  under relation  $r \in \mathcal{R}$ ,  $\mathcal{R}$  indicates the set of different relations,  $W_r^l$  and  $W_0^l$  are trainable parameters,  $\sigma$  is ReLU function.

As the initial input  $h^0$  to the graph encoder, we concatenate a node embedding vector and the averaged word embeddings of node names. Similarly, for each relation  $r$ ,  $E_r$  is the concatenation of a relation embedding vector and the averaged word embeddings of  $r$ ’s label. Both node embedding and relation embedding vectors are randomly initialized and trainable.

To further help our graph encoder to learn with multiple layers of R-GCN, we add highway connections (Srivastava et al., 2015) between layers:

$$\begin{aligned} g &= L^{\text{sigmoid}}(h_i^l), \\ h_i^{l+1} &= g \odot h_i^l + (1 - g) \odot h_i^l, \end{aligned} \quad (3)$$

where  $\odot$  indicates element-wise multiplication.

We use a 6-layer graph encoder, with a hidden size  $H$  of 64 in each layer. The node embedding size is 100, relation embedding size is 32. The number of bases we use is 3.

### A.2. Text Encoder

We use a transformer-based text encoder, which consists of a word embedding layer and a transformer block (Vaswani et al., 2017). Specifically, word embeddings are initialized by the 300-dimensional fastText (Mikolov et al., 2018) word vectors trained on Common Crawl (600B tokens) and kept fixed during training in all settings.

The transformer block consists of a stack of 5 convolutional layers, a self-attention layer, and a 2-layer MLP with a ReLU non-linear activation function in between. In the block, each convolutional layer has 64 filters, each kernel’s size is 5. In the self-attention layer, we use a block hidden size  $H$  of 64, as well as a single head attention mechanism. Layernorm (Ba et al., 2016) is applied after each component inside the block. Following standard transformer training, we add positional encodings into each block’s input.

We use the same text encoder to process text observation  $O_t$  and the action candidate list  $C_t$ . The resulting representations are  $h_{O_t} \in \mathbb{R}^{L_{O_t} \times H}$  and  $h_{C_t} \in \mathbb{R}^{N_{C_t} \times L_{C_t} \times H}$ , where  $L_{O_t}$  is the number of tokens in  $O_t$ ,  $N_{C_t}$  denotes the number of action candidates provided,  $L_{C_t}$  denotes the maximum number of tokens in  $C_t$ , and  $H = 64$  is the hidden size.

### A.3. Representation Aggregator

The representation aggregator aims to combine the text observation representations and graph representations together. Therefore this module is activated only when both the text observation  $O_t$  and the graph input  $\mathcal{G}_t$  are provided. In cases where either of them is absent, for instance, when training the agent with only  $\mathcal{G}^{\text{seen}}$  information, the aggregator will be deactivated and the graph representation will be directly fed into the scorer.

For simplicity, we omit the subscript  $t$  denoting game step in this subsection. At any game step, the graph encoder processes graph input  $\mathcal{G}$ , and generates the graph representation  $h_{\mathcal{G}} \in \mathbb{R}^{N_{\mathcal{G}} \times H}$ . The text encoder processes text observation  $O$  to generate text representation  $h_O \in \mathbb{R}^{L_O \times H}$ .  $N_{\mathcal{G}}$  denotes the number of nodes in the graph  $\mathcal{G}$ ,  $L_O$  denotes the number of tokens in  $O$ .

We adopt a standard representation aggregation method from question answering literature (Yu et al., 2018) to combine the two representations using attention mechanism.

Specifically, the aggregator first uses an MLP to convert both  $h_{\mathcal{G}}$  and  $h_O$  into the same space, the resulting tensors are denoted as  $h'_{\mathcal{G}} \in \mathbb{R}^{N_{\mathcal{G}} \times H}$  and  $h'_O \in \mathbb{R}^{L_O \times H}$ . Then, a trilinear similarity function (Seo et al., 2016) is used to compute the similarities between each token in  $h'_O$  with each node in  $h'_{\mathcal{G}}$ . The similarity between  $i$ th token in  $h'_O$  and  $j$ th node in  $h'_{\mathcal{G}}$  is thus computed by:

$$\text{Sim}(i, j) = W(h'_{O_i}, h'_{\mathcal{G}_j}, h'_{O_i} \odot h'_{\mathcal{G}_j}), \quad (4)$$

where  $W$  is trainable parameters in the trilinear function. By applying the above computation for each pair of  $h'_O$  and  $h'_{\mathcal{G}}$ , a similarity matrix  $S \in \mathbb{R}^{L_O \times N_{\mathcal{G}}}$  is resulted.

Softmax of the similarity matrix  $S$  along both dimensions (number of nodes  $N_{\mathcal{G}}$  and number of tokens  $L_O$ ) are computed, producing  $S_{\mathcal{G}}$  and  $S_O$ . The information contained in the two representations are then aggregated by:

$$\begin{aligned} h_{O\mathcal{G}} &= [h'_O; P; h'_O \odot P; h'_O \odot Q], \\ P &= S_{\mathcal{G}} h'_{\mathcal{G}T}, \\ Q &= S_{\mathcal{G}} S_{OT} h'_{OT}, \end{aligned} \quad (5)$$

where  $h_{O\mathcal{G}} \in \mathbb{R}^{L_O \times 4H}$  is the aggregated observation representation, each token in text is represented by the weighted sum of graph representations. Similarly, the aggregated graph representation  $h_{\mathcal{G}O} \in \mathbb{R}^{N_{\mathcal{G}} \times 4H}$  can also be obtained, where each node in the graph is represented by the weighted sum of text representations. Finally, a linear transformation projects the two aggregated representations to a space with size  $H$  of 64:

$$\begin{aligned} h_{\mathcal{G}O} &= L(h_{\mathcal{G}O}), \\ h_{O\mathcal{G}} &= L(h_{O\mathcal{G}}). \end{aligned} \quad (6)$$

#### A.4. Scorer

The scorer consists of a self-attention layer, a masked mean pooling layer, and a two-layer MLP. As shown in Figure 2 and described above, the input to the scorer is the action candidate representation  $h_{C_t}$ , and one of the following game state representation:

$$s_t = \begin{cases} h_{\mathcal{G}_t} & \text{if only graph input is available,} \\ h_{O_t} & \text{if only text observation is available, this degrades GATA to a Tr-DQN,} \\ h_{\mathcal{G}O_t}, h_{O\mathcal{G}_t} & \text{if both are available.} \end{cases}$$

First, a self-attention is applied to the game state representation  $s_t$ , producing  $\hat{s}_t$ . If  $s_t$  includes graph representations, this self-attention mechanism will reinforce the connection between each node and its related nodes. Similarly, if  $s_t$  includes text representation, the self-attention mechanism strengthens the connection between each token and other related tokens. Further, masked mean pooling is applied to the self-attended state representation  $\hat{s}_t$  and the action candidate representation  $h_{C_t}$ , this results in a state representation vector and a list of action candidate representation vectors. We then concatenate the resulting vectors and feed them into a 2-layer MLP with a ReLU non-linear activation function in between. The second MLP layer has an output dimension of 1, after squeezing the last dimension, the resulting vector is of size  $N_{C_t}$ , which is the number of action candidates provided at game step  $t$ . We use this vector as the score of each action candidate.

#### A.5. Command Generator

The command generator is a transformer-based decoder, it consists of a word embedding layer, a transformer block, and a projection layer.

Similar to the text encoder, the embedding layer is frozen after initializing with the pre-trained fastText word embeddings. Inside the transformer block, there is one self attention layer, two attention layers and a 3-layer MLP with ReLU non-linear activation functions in between. Taking word embedding vectors and the two aggregated representations produced by the representation aggregator as input, the self-attention layer first generates a contextual encoding vectors for the words. These vectors are then fed into the two attention layers to compute attention with graph representations and text observation representations respectively. The two resulting vectors are thus concatenated, and they are fed into the 3-layer MLP. The block hidden size of this transformer is  $H = 64$ .

Finally, the output of the transformer block is fed into the projection layer, which is a linear transformation with output size same as the vocabulary size. The resulting logits are then normalized by a softmax to generate a probability distribution over all words in vocabulary.

During training we utilize the training method of teacher forcing. Specifically, for each step in the sequence generation process, we use the ground-truth target token at previous step as the input. This is in contrast to the “free generation” mode we use during evaluation, where the decoder uses its previously generated token as the input to the model.

Following common practice, we also use a mask to prevent the decoder transformer to access “future” information during training.

## B. Details of Pre-training Tasks and Models

In this section, we start with providing details of the pre-training tasks proposed in Section 4.2 and their corresponding models, and then show these models’ performance for each of the tasks.

Although some of the following pre-training models share certain parts of model structures with GATA, we only load the pre-trained **graph encoder** in all the experiments for fair comparison purposes.

As mentioned in Section 4.2, we use a collection of transitions of the *FTWP* games to carry out the pre-training.

### B.1. Action Prediction (AP)

Given a transition  $(\mathcal{G}_{t-1}, O_{t-1}, C_{t-1}, \mathcal{A}_{t-1}, \mathcal{G}_t, O_t, r_{t-1})$  (as defined in Section 2.1), we use  $\mathcal{A}_{t-1}$  as positive example and use all other action candidates in  $C_{t-1}$  as negative examples. A model is required to identify  $\mathcal{A}_{t-1}$  amongst all action candidates given two consecutive graphs  $\mathcal{G}_{t-1}$  and  $\mathcal{G}_t$ .

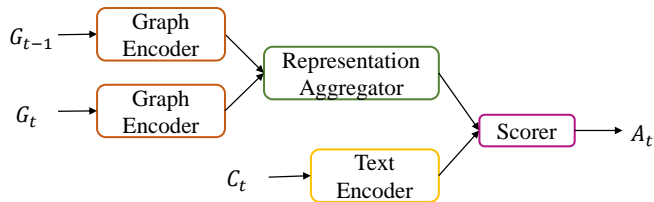


Figure 5. Action Prediction Model.

We use a model with similar structure and components as the action selector of GATA. As illustrated in Figure 5, the graph encoder first converts the two input graphs  $\mathcal{G}_{t-1}$  and  $\mathcal{G}_t$  into hidden representations, the representation aggregator combines them using attention mechanism. The list of action candidates (which includes  $\mathcal{A}_{t-1}$  and all negative examples) are fed into the text encoder to generate action candidate representations. The scorer thus takes these representations and the aggregated graph representations as input, and it outputs a ranking over all action candidates.

In order to achieve good performance in this setting, the bi-directional attention between  $\mathcal{G}_{t-1}$  and  $\mathcal{G}_t$  in the representation aggregator needs to effectively determine the difference between the two sparse graphs. To achieve that, the graph encoder has to extract useful information since often the difference between  $\mathcal{G}_{t-1}$  and  $\mathcal{G}_t$  is minute (e.g., before and after taking an apple from the table, the only change is the location of the apple).

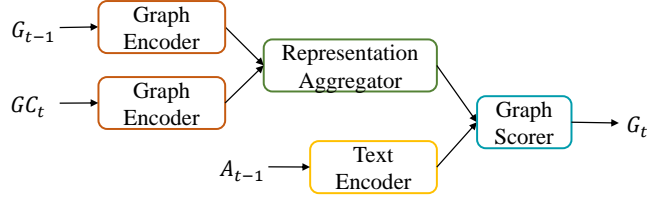


Figure 6. State Prediction Model.

### B.2. State Prediction (SP)

Given a transition  $(\mathcal{G}_{t-1}, O_{t-1}, C_{t-1}, \mathcal{A}_{t-1}, \mathcal{G}_t, O_t, r_{t-1})$ , we use  $\mathcal{G}_t$  as positive example and gather a set of game states by issuing all other actions in  $C_{t-1}$  except  $\mathcal{A}_{t-1}$ . We use the set of graphs representing the resulting game states as negative samples. In this task, a model is required to identify  $\mathcal{G}_t$  amongst all graph candidates  $GC_t$  given the previous graph  $\mathcal{G}_{t-1}$  and the action taken  $\mathcal{A}_{t-1}$ .

As shown in Figure 6, a similar model is used to train both the SP and AP tasks.

### B.3. Deep Graph Infomax (DGI)

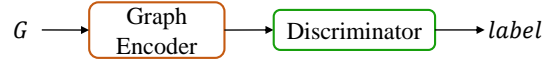


Figure 7. Deep Graph Infomax Model.

Given a transition  $(\mathcal{G}_{t-1}, O_{t-1}, C_{t-1}, \mathcal{A}_{t-1}, \mathcal{G}_t, O_t, r_{t-1})$ , we map the graph  $\mathcal{G}_t$  into its node embedding space. The node embedding vectors of  $\mathcal{G}_t$  is denoted as  $H$ . We randomly shuffle some of the node embedding vectors to construct a “corrupted” version of the node representations, denoted as  $\tilde{H}$ .

Given node representations  $H = \{\vec{h}_1, \vec{h}_2, \dots, \vec{h}_N\}$  and corrupted representations of these nodes  $\tilde{H} = \{\vec{\tilde{h}}_1, \vec{\tilde{h}}_2, \dots, \vec{\tilde{h}}_N\}$ , where  $N$  is the number of vertices in the graph, a model is required to discriminate between the original and corrupted representations of nodes. As shown in Figure 7, the model is composed of a graph encoder and a discriminator. Specifically, following (Veličković et al., 2019), we utilize a noise-contrastive objective with a binary cross-entropy (BCE) loss between the samples from the joint (positive examples) and the product of marginals (negative examples). To enable the discriminator to discriminate between  $\mathcal{G}_t$  and the negative samples, the graph encoder must learn useful graph representations at both global and local level.

### B.4. Command Generation (CG)



Figure 8. Command Generation Model.

The command generation model is exactly the graph updater in GATA. Although both share the same encoder-aggregator topology, the encoders in the graph updater and in the action selector have very different objectives. In order to generate the graph update operation  $\Delta g_t$ , which describes the difference between two consecutive game states, the graph encoder is required to generate proper graph representations that are easily used to determine the *difference* between the graph and text representations. On the other hand, the graph encoder in action selector is required to generate representations that helps to determine the *common* information in graph and text.

Despite having different objectives, the graph encoder trained with command generation task should regardless provide

strong representations. This hypothesis somewhat aligns with the observation (shown in Table 6) that during training, GATA initialized with graph encoder pre-trained on CG generally performs better when *only graph input is available*, compared to using both graph and text observation as input. It is even one of the graph pre-training methods that helps the most during training. However, from Table 7 we do not see the same pattern, where GATA initialized with CG perform significantly worse than the other pre-training methods. This suggests that as a graph representation pre-training task, the CG task provides less generalizability compare to the others.

### B.5. Performance on Pre-training Tasks

We provide test performance of all the four models described above for graph representation learning. We fine-tune the models on validation set and report their performance on test set.

Additionally, as mentioned in Section 3.1 and Appendix A, we adapt the original R-GCN to condition the graph representation on additional information contained by the relation labels. We show an ablation study for this in Table 5, where R-GCN denotes the original R-GCN (Schlichtkrull et al., 2018) and R-GCN w/ R-Emb denotes our version that considers relation labels.

Note, as mentioned in previous sections, the dataset to train, valid and test these four pre-training tasks are extracted from the *FTWP* dataset. There exist unseen nodes (ingredients in recipe) in the validation and test sets of *FTWP*, it requires strong generalizability to get decent performance on these datasets.

From Table 5, we show the relation label representation significantly boosts the generalization performance on these datasets. Compared to AP and SP, where relation label information has significant effect, both models perform near perfectly on the DGI task. This suggests the corruption function we consider in this work is too simple.

Task	Graph Type	R-GCN	R-GCN w/ R-Emb
Accuracy			
AP	full	0.472	<b>0.891</b>
	seen	0.631	<b>0.873</b>
SP	full	0.419	<b>0.926</b>
	seen	0.612	<b>0.971</b>
DGI	full	0.999	<b>1.000</b>
	seen	<b>1.000</b>	<b>1.000</b>
F <sub>1</sub> Score			
CG	seen	0.910	<b>0.968</b>

Table 5. Test performance of models on all pre-training tasks.

## C. More Results

### C.1. Training Curves

We report GATA’s and text-based baselines’ training curves in all setting and all pre-training strategies. Figure 9 shows the settings where we load-and-freeze the pre-trained graph encoder. Figure 10 shows the settings where we load-and-fine-tune the pre-trained graph encoder.

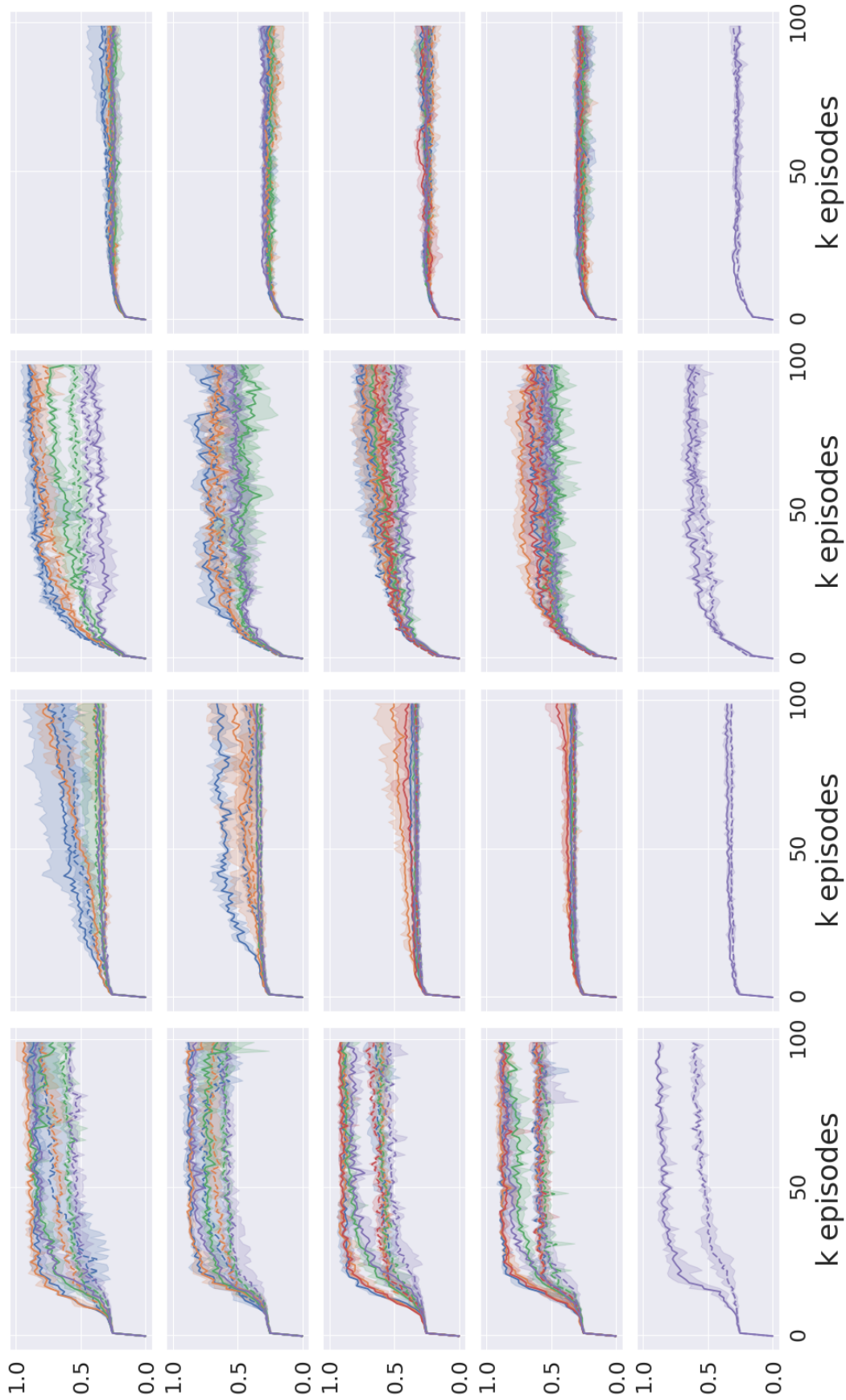


Figure 9. GATA’s training curves (averaged over 3 seeds, band represents standard deviation), **load-and-freeze** pre-trained graph encoder. Columns are difficulty levels 1/2/3/4, rows 1-4 show performance of GATA with  $\blacklozenge$  /  $\blacklozenge$  /  $\blacklozenge$  /  $\blacklozenge$  /  $\blacklozenge$  as input, the 5th row shows performance of Tr-DQN.  $\blacklozenge$  :  $\mathcal{G}^{\text{full}}$ ,  $\blacklozenge$  :  $\mathcal{G}^{\text{seen}}$ ,  $\blacklozenge$  : text. For GATA, colored lines represent the agent use a graph encoder pre-trained on **Random/AP/SP/DGI/CG** task. Note the Tr-DQN agent (5th row) does not have graph component. Solid lines represent training size 20, dashed lines represent training size of 100.

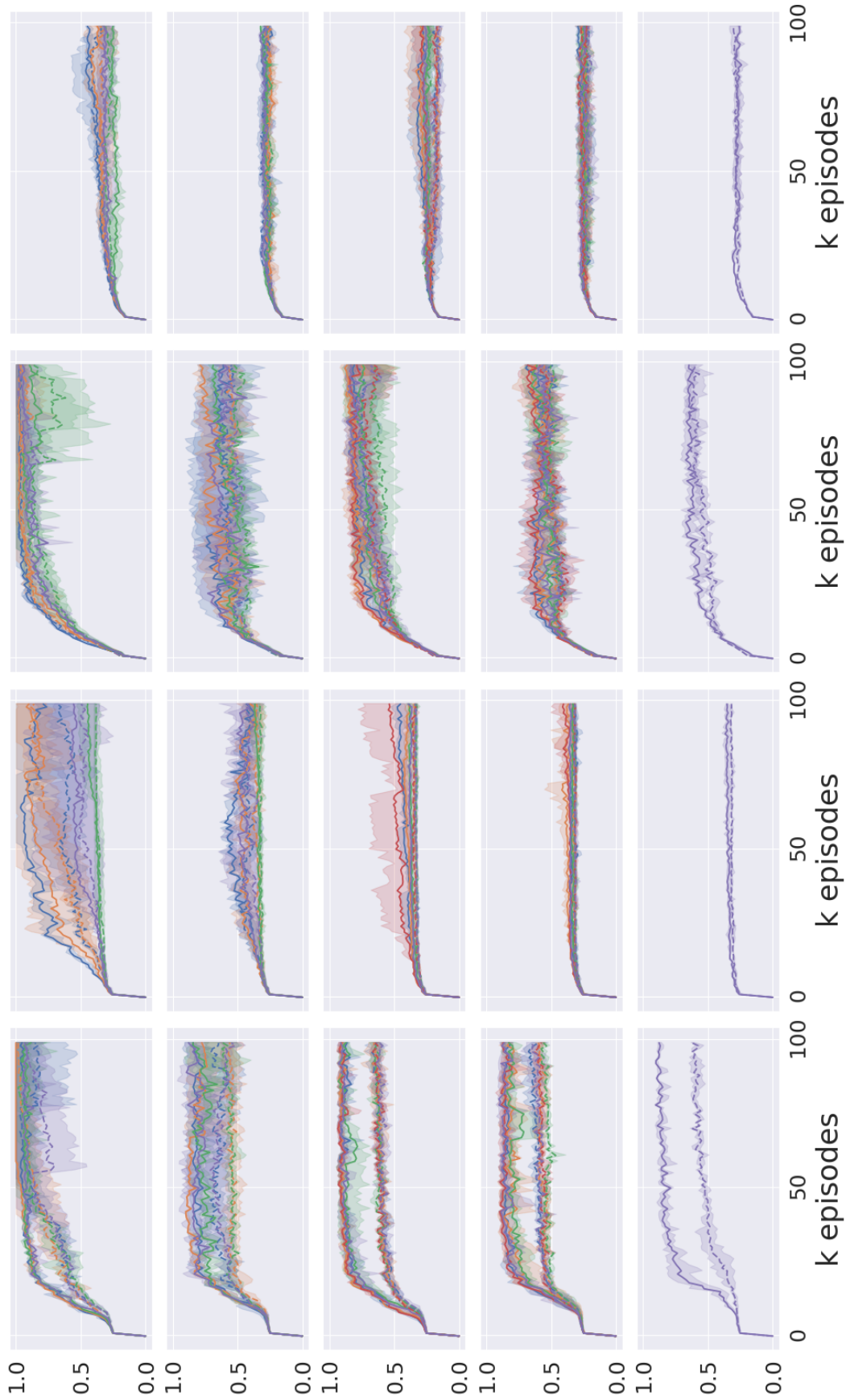


Figure 10. GATA’s training curves (averaged over 3 seeds, band represents standard deviation), **load-and-finetune** pre-trained graph encoder. Columns are difficulty levels 1/2/3/4, rows 1-4 show performance of GATA with  $\blacklozenge/\blacklozenge/\blacklozenge/\blacklozenge$  as input, the 5th row shows performance of Tr-DQN.  $\blacklozenge$  :  $\mathcal{G}^{\text{full}}$ ,  $\blacklozenge$  :  $\mathcal{G}^{\text{seen}}$ . For GATA, colored lines represent the agent use a graph encoder pre-trained on **Random/AP/SP/DG/CG** task. Note the Tr-DQN agent (5th row) does not have graph component. Solid lines represent training size 20, dashed lines represent training size of 100.

## C.2. Training Scores

In Table 6 we provide all agents’ max training scores, each score is averaged over 3 random seeds. All scores are normalized. Note as described in Section 4.1, we use ground-truth KGs to train the action selector,  $\mathcal{G}^{\text{belief}}$  is only used during evaluation.

		20 Training Games					100 Training Games					Avg.
Difficulty Level		1	2	3	4	% ↑	1	2	3	4	% ↑	% ↑
Input	Agent	Baseline: Without Graph Encoder										
♣	Tr-DQN	90.8	36.9	69.3	31.5	—	63.4	33.2	66.1	31.9	—	—
♣	Tr-DRQN	88.8	41.7	76.6	29.6	+3.8	60.8	33.7	71.7	30.6	+0.5	+2.1
♣	Tr-DRQN+	89.1	35.6	78.0	30.9	+1.3	61.1	32.8	70.0	30.0	-1.2	+0.0
Pre-training		Load-and-Freeze Pre-trained Graph Encoder										
♦	AP	92.0	77.1	93.0	37.3	+40.7	85.3	67.5	92.6	35.2	+47.1	+43.9
♦	SP	95.3	80.8	91.5	31.3	+38.8	83.0	41.7	85.8	31.2	+21.0	+29.9
♦	DGI	92.6	37.8	77.9	28.4	+1.7	66.6	40.9	60.6	28.5	+2.3	+2.0
♦♣	AP	91.2	70.7	87.5	32.4	+30.3	80.7	50.7	77.7	31.5	+24.1	+27.2
♦♣	SP	90.6	54.5	79.6	31.5	+15.6	75.3	45.0	73.2	30.4	+15.1	+15.3
♦♣	DGI	79.4	36.4	60.6	28.6	-8.9	64.1	33.3	57.8	29.0	-5.1	-7.0
♥	AP	92.7	39.1	83.2	33.6	+8.7	67.4	34.0	77.2	29.1	+4.2	+6.4
♥	SP	94.2	56.6	77.5	28.8	+15.1	64.7	34.4	68.4	26.3	-2.1	+6.5
♥	DGI	92.9	37.3	71.4	31.4	+1.5	64.8	33.8	57.0	27.4	-6.0	-2.2
♥	CG	94.2	44.1	68.0	33.1	+6.6	72.5	34.7	63.0	29.2	+1.4	+4.0
♥♣	AP	91.2	36.7	72.6	33.1	+2.4	65.9	33.4	63.6	30.4	-1.0	+0.7
♥♣	SP	91.7	39.9	80.0	32.7	+7.1	64.2	35.4	67.1	29.8	+0.7	+3.9
♥♣	DGI	88.1	35.5	58.8	31.0	-5.9	61.1	33.3	55.4	29.8	-6.5	-6.2
♥♣	CG	90.7	46.6	72.6	31.9	+8.1	64.6	33.7	63.2	31.2	-0.8	+3.6
Pre-training		Load-and-Fine-Tune Pre-trained Graph Encoder										
♦	N/A	98.6	58.4	95.6	36.1	+29.9	96.0	53.4	97.9	36.0	+43.3	+36.6
♦	AP	98.7	97.5	98.3	48.1	+66.9	97.1	74.7	98.3	44.5	+66.6	+66.7
♦	SP	100.0	96.9	98.3	44.9	+64.3	98.6	90.5	99.0	38.9	+75.0	+69.6
♦	DGI	96.9	45.4	95.3	28.7	+14.6	98.2	39.1	90.1	33.0	+28.1	+21.4
♦♣	N/A	91.7	55.9	80.9	33.6	+19.0	73.5	48.1	67.7	31.8	+15.7	+17.4
♦♣	AP	87.9	62.4	78.8	32.4	+20.6	76.8	54.0	73.7	34.1	+25.5	+23.1
♦♣	SP	90.7	55.8	83.8	30.7	+17.4	60.4	40.1	67.4	31.1	+3.9	+10.6
♦♣	DGI	88.1	38.1	73.0	32.5	+2.2	66.4	35.5	59.1	30.4	-0.9	+0.6
♥	N/A	94.3	39.9	88.2	31.0	+9.4	65.2	35.0	81.9	26.5	+3.8	+6.6
♥	AP	94.0	48.9	86.5	35.0	+18.0	70.9	34.8	81.7	25.6	+5.1	+11.6
♥	SP	93.3	43.6	89.6	33.5	+14.1	68.5	35.5	88.1	26.2	+7.6	+10.9
♥	DGI	94.2	39.7	81.2	29.6	+5.6	69.3	34.5	69.8	28.6	+2.1	+3.9
♥	CG	94.0	55.8	86.2	32.1	+20.3	69.0	37.1	77.7	26.3	+5.1	+12.7
♥♣	N/A	91.6	37.0	68.1	31.1	-0.5	66.8	32.9	63.0	28.1	-3.0	-1.7
♥♣	AP	89.3	36.7	74.8	31.2	+1.2	68.7	33.1	60.2	29.9	-1.8	-0.3
♥♣	SP	89.8	43.3	71.5	29.4	+3.2	64.2	34.5	59.9	30.5	-2.1	+0.5
♥♣	DGI	87.0	35.3	65.9	30.0	-4.5	60.1	33.3	57.4	29.5	-6.4	-5.5
♥♣	CG	90.6	42.1	76.3	30.1	+4.9	63.7	33.1	61.1	30.7	-2.8	+1.0

Table 6. Agents’ Max performance on **Training** games, averaged over 3 random seeds. In this table, ♣, ♦ and ♥ represent  $O_t$ ,  $\mathcal{G}_t^{\text{full}}$  and  $\mathcal{G}_t^{\text{seen}}$  respectively. Light blue shadings represent numbers that are greater than or equal to Tr-DQN; light yellow shading represent number that are greater than or equal to all of Tr-DQN, Tr-DRQN and Tr-DRQN+.

## C.3. Test Results

In Table 7 we provide the text-based baselines and GATA-GT’s test scores. In Table 8 we provide the text-based baselines and GATA’s test scores. We report agents’ test score corresponding to their best validation scores.

		20 Training Games					100 Training Games					Avg.
Difficulty Level		1	2	3	4	% ↑	1	2	3	4	% ↑	% ↑
Input	Agent	Baseline: Without Graph Encoder										
♣	Tr-DQN	66.2	26.0	16.7	18.2	—	62.5	32.0	38.3	17.7	—	—
♣	Tr-DRQN	62.5	32.0	28.3	12.7	+14.2	58.8	31.0	36.7	21.4	+1.9	+8.1
♣	Tr-DRQN+	65.0	30.0	35.0	11.8	+22.0	58.8	33.0	33.3	19.5	-1.4	+10.3
Pre-training		Load-and-Freeze Pre-trained Graph Encoder (With Ground-truth Graph)										
♦	AP	66.2	38.0	41.7	22.3	+54.6	85.0	81.0	60.0	27.7	+75.6	+65.1
♦	SP	66.2	28.0	25.0	20.0	+16.8	70.0	54.0	36.7	21.4	+24.4	+20.6
♦	DGI	42.5	28.0	30.0	14.5	+7.8	58.8	65.0	36.7	15.5	+20.1	+14.0
♦♣	AP	68.8	43.0	36.7	23.2	+54.1	81.2	46.0	51.7	27.7	+41.3	47.7
♦♣	SP	61.3	48.0	33.3	21.8	+49.1	88.7	48.0	31.7	27.3	+32.2	40.7
♦♣	DGI	70.0	32.0	21.7	11.4	+5.3	70.0	30.0	28.3	11.4	-14.0	-4.3
♥	AP	62.5	23.0	21.7	23.2	+10.1	66.2	32.0	53.3	20.9	+15.8	+12.9
♥	SP	58.8	25.0	30.0	14.1	+10.5	65.0	30.0	36.7	19.5	+0.9	+5.7
♥	DGI	60.0	24.0	21.7	10.9	-6.8	57.5	31.0	35.0	14.1	-10.0	-8.4
♥	CG	41.2	24.0	13.3	13.2	-23.3	62.5	31.0	40.0	15.9	-2.2	-12.8
♥♣	AP	66.2	32.0	28.3	13.6	+16.8	58.8	31.0	38.3	16.4	-4.1	+6.4
♥♣	SP	58.8	32.0	26.7	21.4	+23.3	62.5	33.0	41.7	14.1	-2.1	+10.1
♥♣	DGI	70.0	35.0	30.0	14.1	+24.4	51.2	31.0	28.3	12.3	-19.5	+2.5
♥♣	CG	62.5	32.0	15.0	15.9	-1.3	66.2	34.0	36.7	24.1	+11.0	+4.9
Pre-training		Load-and-Fine-Tune Pre-trained Graph Encoder (With Ground-truth Graph)										
♦	N/A	83.8	53.0	33.3	23.6	+64.9	100.0	90.0	68.3	37.3	+107.6	+86.2
♦	AP	85.0	39.0	26.7	26.4	+45.8	92.5	88.0	63.3	53.6	+122.8	+84.3
♦	SP	48.7	61.0	46.7	23.6	+79.4	95.0	95.0	70.0	37.3	+110.6	+95.0
♦	DGI	85.0	27.0	31.7	14.1	+24.9	100.0	40.0	70.0	31.8	+61.9	+43.4
♦♣	N/A	92.5	39.0	30.0	15.9	+39.2	96.3	56.0	55.0	14.5	+38.7	+38.9
♦♣	AP	73.8	36.0	46.7	25.9	+68.0	85.0	42.0	68.3	36.4	+62.8	+65.4
♦♣	SP	62.5	24.0	36.7	14.5	+21.5	60.0	43.0	46.7	25.0	+23.4	+22.5
♦♣	DGI	81.2	30.0	25.0	16.8	+20.0	73.8	39.0	48.3	15.0	+12.7	+16.4
♥	N/A	60.0	24.0	38.3	15.0	+23.7	61.3	33.0	41.7	25.5	+13.5	+18.6
♥	AP	65.0	28.0	28.3	11.4	+9.5	62.5	28.0	56.7	27.7	+23.0	+16.3
♥	SP	60.0	34.0	30.0	19.1	+26.5	58.8	33.0	43.3	30.9	+21.2	+23.9
♥	DGI	57.5	14.0	26.7	7.7	-14.3	73.8	31.0	38.3	22.7	+10.8	-1.7
♥	CG	61.3	29.0	23.3	20.0	+13.4	65.0	34.0	40.0	18.2	+4.4	+8.9
♥♣	N/A	73.8	27.0	35.0	15.9	+28.1	58.8	33.0	41.7	15.0	-2.3	+12.9
♥♣	AP	58.8	33.0	35.0	17.7	+30.6	62.5	32.0	45.0	21.4	+9.6	+20.1
♥♣	SP	58.8	26.0	30.0	20.9	+20.8	58.8	32.0	28.3	20.0	-4.8	+8.0
♥♣	DGI	68.8	32.0	41.7	13.6	+37.9	62.5	34.0	41.7	15.5	+0.7	+19.3
♥♣	CG	68.8	26.0	36.7	10.0	+19.7	66.2	32.0	35.0	12.7	-7.7	+6.0

Table 7. Agents’ performance on **Test** games, model selected using best validation performance. In this table, ♣, ♦ and ♥ represent  $O_t$ ,  $G_t^{\text{full}}$  and  $G_t^{\text{seen}}$  respectively. Light blue shadings represent numbers that are greater than or equal to Tr-DQN; light yellow shading represent number that are greater than or equal to all of Tr-DQN, Tr-DRQN and Tr-DRQN+.

Learning Dynamic Knowledge Graphs to Generalize on Text-based Games

		20 Training Games					100 Training Games					Avg.
Difficulty Level		1	2	3	4	% ↑	1	2	3	4	% ↑	% ↑
Input	Agent	Baseline: Without Graph Encoder										
♣	Tr-DQN	66.2	26.0	16.7	18.2	—	62.5	32.0	38.3	17.7	—	—
♣	Tr-DRQN	62.5	32.0	28.3	12.7	+14.2	58.8	31.0	36.7	21.4	+1.9	+8.1
♣	Tr-DRQN+	65.0	30.0	35.0	11.8	+22.0	58.8	33.0	33.3	19.5	-1.4	+10.3
Pre-training		Load-and-Freeze Pre-trained Graph Encoder										
♣	AP	62.5	21.0	20.0	17.3	-2.5	<u>66.2</u>	31.0	<b>56.7</b>	18.6	+14.0	+5.7
♣	SP	58.8	22.0	30.0	13.2	+6.4	<u>65.0</u>	27.0	30.0	16.8	-9.6	-1.6
♣	DGI	60.0	25.0	21.7	8.2	-9.6	53.7	31.0	25.0	9.5	-24.6	-17.1
♣	CG	45.0	22.0	08.3	8.6	-37.6	<u>66.2</u>	26.0	35.0	13.2	-11.7	-24.7
♣ ♠	AP	62.5	20.0	21.7	17.3	-0.9	62.5	31.0	<u>53.3</u>	19.1	+11.0	+5.0
♣ ♠	SP	60.0	24.0	30.0	13.6	+9.3	65.0	28.0	36.7	17.7	-3.2	+3.1
♣ ♠	DGI	60.0	24.0	20.0	09.1	-11.8	55.0	28.0	20.0	13.6	-23.9	-17.8
♣ ♠	CG	37.5	22.0	16.7	09.5	-26.6	<b>70.0</b>	28.0	40.0	14.1	-4.1	-15.4
♣ ♠	AP	<u>66.2</u>	30.0	30.0	11.8	+15.0	62.5	32.0	33.3	17.3	-3.8	+5.6
♣ ♠	SP	58.8	31.0	25.0	20.0	+16.9	62.5	<u>35.0</u>	41.7	15.0	+0.7	+8.8
♣ ♠	DGI	62.5	<u>35.0</u>	30.0	14.1	+21.5	51.2	32.0	23.3	11.8	-22.6	-0.6
♣ ♠	CG	62.5	<u>33.0</u>	15.0	15.5	-0.9	<b>70.0</b>	33.0	38.3	25.0	+14.1	+6.6
♣ ♠	AP	<u>66.2</u>	30.0	31.7	13.2	+19.4	58.8	32.0	38.3	16.8	-2.8	+8.3
♣ ♠	SP	58.8	32.0	26.7	20.0	+20.4	62.5	<b>36.0</b>	41.7	15.0	+1.5	+11.0
♣ ♠	DGI	<u>66.2</u>	<u>35.0</u>	30.0	12.3	+20.5	51.2	29.0	23.3	11.8	-25.0	-2.3
♣ ♠	CG	62.5	<u>33.0</u>	15.0	15.9	-0.4	62.5	34.0	38.3	25.0	+1.9	+5.8
Pre-training		Load-and-Fine-Tune Pre-trained Graph Encoder										
♣	N/A	58.8	21.0	36.7	14.5	+17.3	57.5	30.0	35.0	25.5	+5.3	+11.3
♣	AP	65.0	30.0	23.3	10.0	+2.0	58.8	26.0	43.3	28.2	+11.9	+7.0
♣	SP	60.0	26.0	25.0	13.6	+3.8	58.8	33.0	40.0	28.2	+15.2	+9.5
♣	DGI	42.5	12.0	25.0	10.9	-20.0	<u>66.2</u>	28.0	41.7	19.1	+2.6	-8.7
♣	CG	51.2	<b>36.0</b>	21.7	15.9	+8.3	58.8	33.0	30.0	15.9	-8.7	-0.2
♣ ♠	N/A	65.0	24.0	33.3	15.9	+19.3	62.5	30.0	45.0	26.4	+15.1	+17.2
♣ ♠	AP	65.0	29.0	28.3	9.5	+7.8	<u>66.2</u>	25.0	50.0	<b>29.5</b>	<b>+20.3</b>	+14.1
♣ ♠	SP	61.3	30.0	25.0	11.4	+5.1	58.8	33.0	45.0	<u>28.6</u>	+19.1	+12.1
♣ ♠	DGI	55.0	13.0	25.0	10.9	-14.3	<b>70.0</b>	30.0	43.3	20.0	+7.9	-3.2
♣ ♠	CG	60.0	24.0	23.3	16.4	+3.1	<u>66.2</u>	32.0	40.0	16.4	+0.8	+1.9
♣ ♠	N/A	<b>73.8</b>	26.0	35.0	15.0	+25.9	62.5	33.0	36.7	14.1	-5.3	+10.3
♣ ♠	AP	58.8	30.0	35.0	18.2	+28.4	62.5	32.0	51.7	18.6	+10.0	+19.2
♣ ♠	SP	58.8	25.0	33.3	20.5	+24.3	58.8	32.0	31.7	18.2	-5.1	+9.6
♣ ♠	DGI	<u>68.8</u>	31.0	40.0	15.9	+37.5	62.5	34.0	36.7	15.5	-2.6	+17.5
♣ ♠	CG	65.0	24.0	<u>36.7</u>	10.9	+17.5	62.5	32.0	35.0	13.2	-8.5	+4.5
♣ ♠	N/A	<b>73.8</b>	25.0	35.0	15.5	+25.6	58.8	33.0	36.7	14.1	-6.8	+9.4
♣ ♠	AP	58.8	32.0	38.3	16.8	+33.4	62.5	32.0	48.3	20.0	+9.8	+21.6
♣ ♠	SP	58.8	26.0	35.0	<b>20.9</b>	+28.3	58.8	32.0	28.3	19.5	-5.5	+11.4
♣ ♠	DGI	<u>68.8</u>	33.0	<b>41.7</b>	14.1	+39.2	62.5	34.0	36.7	15.5	-2.6	+18.5
♣ ♠	CG	<u>68.8</u>	23.0	36.7	11.8	+19.2	<b>70.0</b>	32.0	40.0	12.7	-3.0	+8.1

Table 8. Agents’ performance on **Test** games, model selected using best validation performance. **Boldface** and underline represent the highest and second highest values in a setting. In this table, ♣ and ♠ represent  $O_t$  and  $G_t^{\text{belief}}$  respectively, ■ indicates the graph updater is fine-tuned on the fly. Light blue shadings represent numbers that are greater than or equal to Tr-DQN; light yellow shading represent number that are greater than or equal to all of Tr-DQN, Tr-DRQN and Tr-DRQN+.

#### C.4. Other Remarks

**Fine-tuning graph encoder helps.** For all experiment settings, we also compare between freezing vs. fine-tuning the graph encoder in the action selector after loading pre-trained parameters. The initial rationale behind is, it is possible the graph encoder has been pre-trained enough, and by freezing the parameters we can effectively reduce the number of parameters to be optimized with RL signal. However, we see consistent trends that fine-tuning graph encoder can always provide better performance during both training and testing (Tables 6, 7, 8).

**Fine-tuning graph updater helps.** We also investigate whether fine-tuning the graph updater helps. We observe minor improvement (Tables 6, 7, 8). During the pre-training of graph updater, we use transitions extracted from the *FTWP* games with *mixed* difficulty levels, whereas we train and test action selector on different difficulty levels *separately*. Therefore, this fine-tuning may enable the graph updater to adapt to the new game distributions by learning useful task specific information (e.g., in level 1 games there is only a single location, the graph updater can focus less on graph updates for navigation).

**DGI works better together with text.** We observe that during zero-shot testing, GATA initialized with DGI often works significantly better when text observation is jointly used with the graph as input to the action selector. We suspect this is related to the special properties of the DGI pre-training task since it is the only task without involving text information. Different from the DGI pre-training task, when playing text-based games, an agent’s decision making process is conditioned on the representations of action candidates. Thus, pre-training tasks other than DGI may have learned to generate graph representations that are easier to integrate with text representations since they all have text information involved.

**Text input helps more when graphs are imperfect.** We observe clear trends that for GATA-GT, using text together with graph as input does not provide obvious performance increase. Instead, GATA-GT often show better performance when text observation input is disabled. Although, as mentioned in Section 2.1, when the graph updater is perfect,  $\mathcal{G}^{\text{belief}} = \mathcal{G}^{\text{seen}}$ . However, practically, the graph updater might generate wrong connections or overlook certain state changes. Under such circumstances, we expect the text observation input to be more useful. Results shown in Table 8 support our hypothesis, where when GATA uses the (sometimes imperfect)  $\mathcal{G}^{\text{belief}}$  extracted and updated by itself, the text observation input can provide a boost compared to only using  $\mathcal{G}^{\text{belief}}$ .

**What happened on level 1 games?** On level 1 games, we observe that GATA-GT with  $\mathcal{G}^{\text{full}}$  sometimes perform worse compare to the other agents, even the text-based baselines. As shown in Table 2, level 1 games have only a single location. This makes both  $O_t$  and  $\mathcal{G}^{\text{seen}}$  very close to  $\mathcal{G}^{\text{full}}$  (the only difference might be information described in the recipe, which an agent needs to read). Moreover, recipes in level 1 games only require a single ingredient to be processed, this is relatively easier for an agent to gather knowledge by exhausting the environment (i.e., in such case, a text-based agent may abuse the simpleness of level 1 games and learn a brute force policy). We suspect this is due to different properties between text and graph input modalities. Text is abstractive and uncertain, however it is easier to distinguish between different pieces of text. In contrast, graphs represents knowledge in a more certain way, but the difference between similar graphs is relatively harder to capture. When an environment is simple, optimization methods such as deep Q-Learning can easily learn by memorising input-action pairs after actions are randomly explored. In this case, input modalities that are more distinguishable might be easier to be “learned”. However, in harder games, where an accurate representation of the world is required (i.e., level 2, 3, 4), graph inputs show significant advantage compared to text.

#### C.5. Future Directions

**Better Policies** We show that GATA can achieve a generalization performance close to GATA-GT with  $\mathcal{G}^{\text{seen}}$ . This suggests the proposed graph extracting and updating method is providing high quality graph inputs to our agent. However, on most settings, we observe huge gap between GATA with GATA-GT with  $\mathcal{G}^{\text{full}}$ . This is because GATA’s performance still relies heavily on its policies. Although the extracted KGs almost helps GATA to achieve the upper-bound information it can obtain from experienced moves, it remains difficult when GATA cannot visit informative locations. One interesting direction is to develop a mechanism to encourage exploration which conditions on the maintained KG.

**Better Representation Learning Methods** In this work, we show four different graph representation learning methods, in which AP and SP constantly help GATA to achieve better performance and generalization. More work can be explored along this line. For instance, we observe a graph encoder performs worse when pre-trained on the DGI task, this may

because its pre-training process does not involve the synergy between graph representations and text representations. It would be interesting to consider contrastive predictive representation learning tasks across modalities.

## D. Implementation Details

In Appendix A, we have introduced hyperparameters regarding model structures. In this section, we provide hyperparameters we used in training and optimizing.

In all experiments, we use *Rectified Adam* (Liu et al., 2019) as the step rule for optimization, The learning rate is set to 0.001. We clip gradient norm of 5.

### D.1. Action Selector

We use a prioritized replay buffer with memory size of 500,000, and a priority fraction of 0.6. During playing the game, we use batch size of 1. We use  $\epsilon$ -greedy, where the value of  $\epsilon$  anneals from 1.0 to 0.1 within 20,000 episodes. We start updating parameters after 100 episodes of playing. We update our network after every 50 game steps (update frequency  $F$  in Algorithm 1). During update, we use a mini-batch of size 64. We use a discount  $\gamma = 0.9$ . We update target network after every 500 episodes. For multi-step learning, we sample the multi-step return  $n \sim \text{Uniform}[1, 3]$ . We refer readers to Hessel et al. (2017) for more information about different components of DQN training.

In our implementation of Tr-DRQN and Tr-DRQN+ baselines, following Yuan et al. (2018), we sample a sequence of transitions of length 8, use the first 4 transitions to estimate reasonable recurrent states and use the last for to update. For counting bonus, we use a  $\gamma_c = 0.5$ , the bonus is scaled by an coefficient  $\lambda_c = 0.1$ .

For all experiment settings, we train agents for 100,000 episodes (NB\_EPISODES in Algorithm 1). For each game, we set maximum step of 50 (NB\_STEPS in Algorithm 1). When an agent has used up all its moves, the game is forced to terminate. We evaluate them after every 1,000 episodes (evaluation frequency  $E$  in Algorithm 1). Patience  $P$  and tolerance  $\tau$  in Algorithm 1 are 3 and 0.1, respectively. The agents are implemented using PyTorch (Paszke et al., 2017). The training process of every agent takes approximately 2 days on a single NVIDIA P100 GPU.

### D.2. Graph Updater

During training, we use a batch size of 128. During evaluation, we set the maximum number of tokens to be 100. Specifically, the graph updater starts from a special token  $\langle \text{begin-of-sequence} \rangle$  and uses the generated token at previous step as the input to the transformer decoder, until generating another special token  $\langle \text{end-of-sequence} \rangle$  or exhausting the maximum number of tokens. The convergence takes approximately 2 days on a single NVIDIA P100 GPU.

### D.3. Pre-training Graph Encoder

To fit the needs of different experimental settings in Section 5, we train the following 7 different models.

1. AP with  $\mathcal{G}^{\text{full}}$ : batch size is 256, the convergence takes approximately 2 days on a single NVIDIA P40 GPU.
2. AP with  $\mathcal{G}^{\text{seen}}$ : batch size is 256, the convergence takes approximately 2 days on a single NVIDIA P40 GPU.
3. SP with  $\mathcal{G}^{\text{full}}$ : batch size is 48, the convergence takes approximately 5 days on a single NVIDIA P40 GPU.
4. SP with  $\mathcal{G}^{\text{seen}}$ : batch size is 48, the convergence takes approximately 5 days on a single NVIDIA P40 GPU.
5. DGI with  $\mathcal{G}^{\text{full}}$ : batch size is 256, the convergence takes approximately a day on a single NVIDIA P40 GPU.
6. DGI with  $\mathcal{G}^{\text{seen}}$ : batch size is 256, the convergence takes approximately a day on a single NVIDIA P40 GPU.
7. CG with  $\mathcal{G}^{\text{seen}}$ : batch size is 128, the convergence takes approximately 2 days on a single NVIDIA P40 GPU.

Note there is no CG pre-training on  $\mathcal{G}^{\text{full}}$ , because for fully observed graphs, all the information is already given. Maintaining such graph only involves a few operations (e.g., if a player moves to a new location, the graph should only update the player’s location information, rather than all information about the new location), thus the resulting task may be trivial.

### E. Extracting Ground-truth Graphs from TextWorld Games

Under the hood, TextWorld relies on predicate logic to handle the game dynamics. Therefore, the underlying game state consists of a set of predicates, and logic rules (i.e. actions) can be applied to update them. TextWorld’s API allows us to obtain such underlying state  $S_t$  at a given game step  $t$  for any games generated by the framework. We leverage  $S_t$  to extract both  $\mathcal{G}_t^{\text{full}}$  and  $\mathcal{G}_t^{\text{seen}}$ . Figure 11 shows an example of consecutive  $\mathcal{G}_t^{\text{seen}}$  as the agent explores the environment of a level-4 game. Figure 12 shows the  $\mathcal{G}^{\text{full}}$  extracted from the same game.

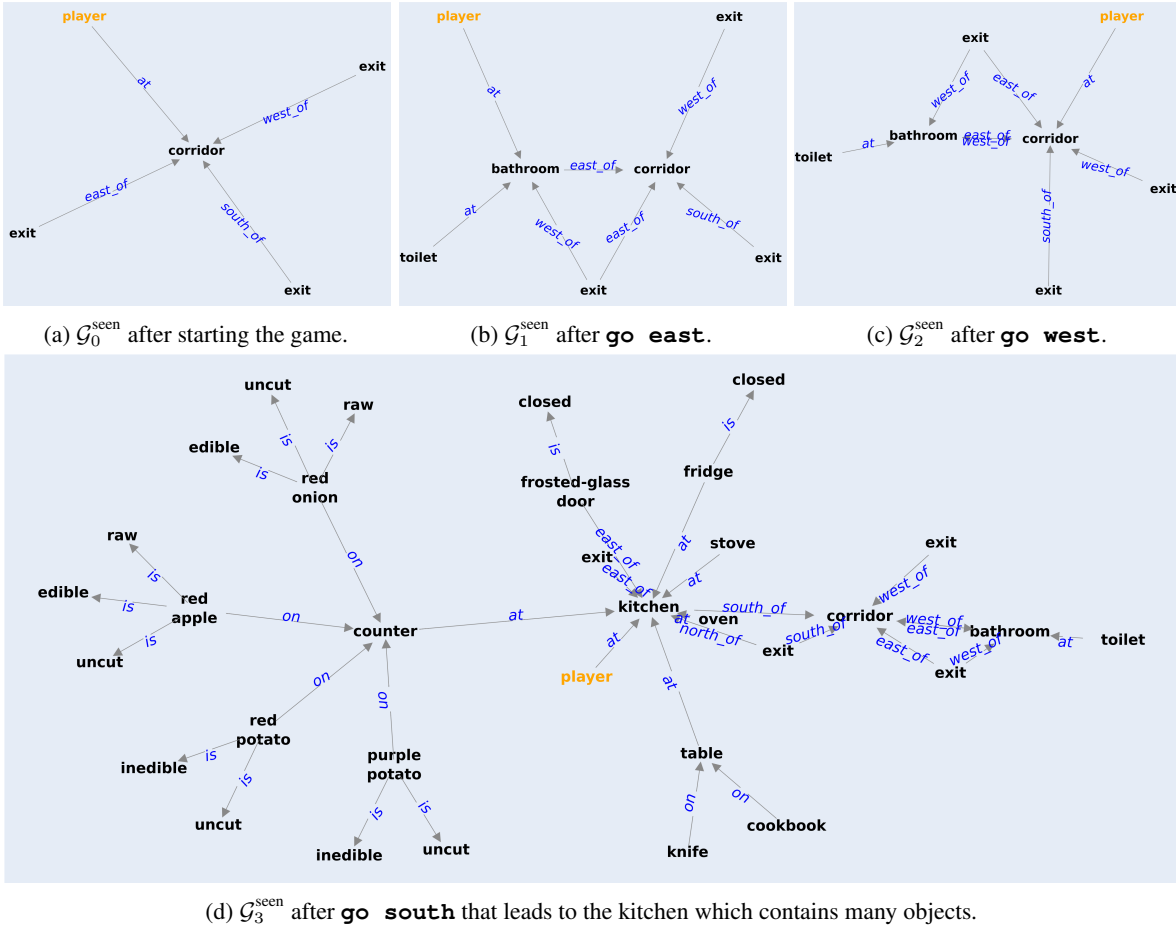


Figure 11. A sequence of  $\mathcal{G}^{\text{seen}}$  extracted after issuing three consecutive actions in a level-4 game.

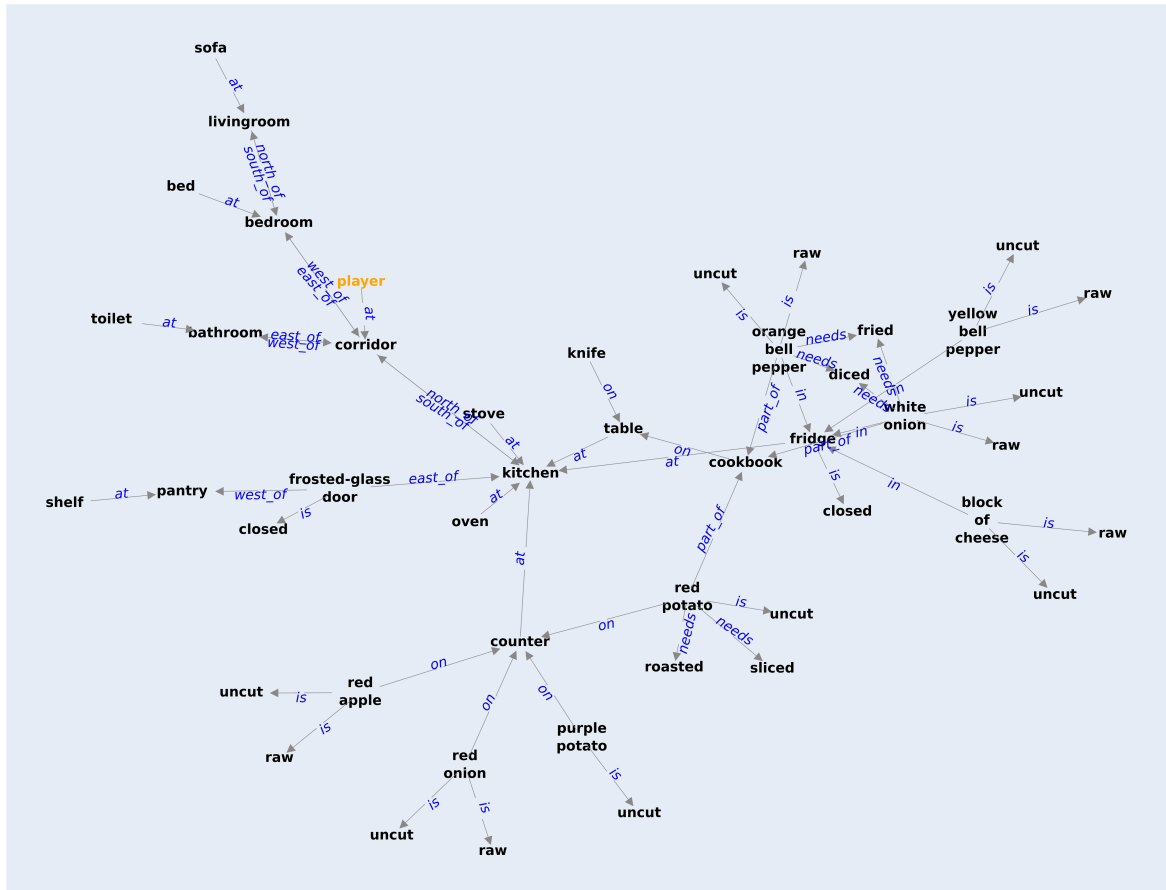


Figure 12.  $\mathcal{G}^{\text{full}}$  at the start of a level-4 game.